# Silicate Melts & Glasses: Chemical Diffusion, Nucleation & Crystallization, Interrelated

Reid F. Cooper
Department of Geological Sciences
Brown University

***Acknowledgements:*** Glen Cook, John Fanselow, Donald Smith, Rebecca Everman, Claire Pettersen, Katherine Burgess

***Foundation*:**

C. Wagner, Reaktionstypen bei der oxydation von legierungen, *Z. Elektrochemie,* **63**, 772 (1959).

H. Schmalzried, Internal & external oxidation of nonmetallic compounds and solid solutions (I), *Ber. Bunsenges. Phys. Chem.* **87**, 1186–1191 (1983).

G.B. Cook & R.F. Cooper, Iron concentration & the physical processes of dynamic oxidation in an alkaline earth aluminosilicate glass, *Am. Mineral.* **85**, 397–406 (2000).

P.C. Hess, Polymerization model for silicate melts, in *Physics of Magmatic Processes*, R.B. Hargraves, ed., Princeton Univ. Press (1980).


***Rowland Cannon Memorial International Workshop on Interfaces in Functional Materials; Macungie, PA; 13 October 2006***

# Phenomena of Interest—and Questions

- **Stability of transition-metal cation-bearing glasses or melts as a function of cation valence and the consequent relationship between melt structure and liquidus phase.**
- **Kinetic mechanisms of oxidation and reduction in these systems.**
- **Texture or ”Reaction Morphology”—the spatial distribution of elements and phases that result from a reaction—as evidence of the mechanism(s) dominating the reaction.**

  $\longrightarrow$ **Interrelated: cf. Wagner/Schmalzried Theory of Oxidation**

- **Discerning the role(s) kinetic mechanisms play in in establishing a “persistent” metastability.**

BROWN

# Thermodynamics of Nucleation: $|\Delta_{rxn}G| > 0$

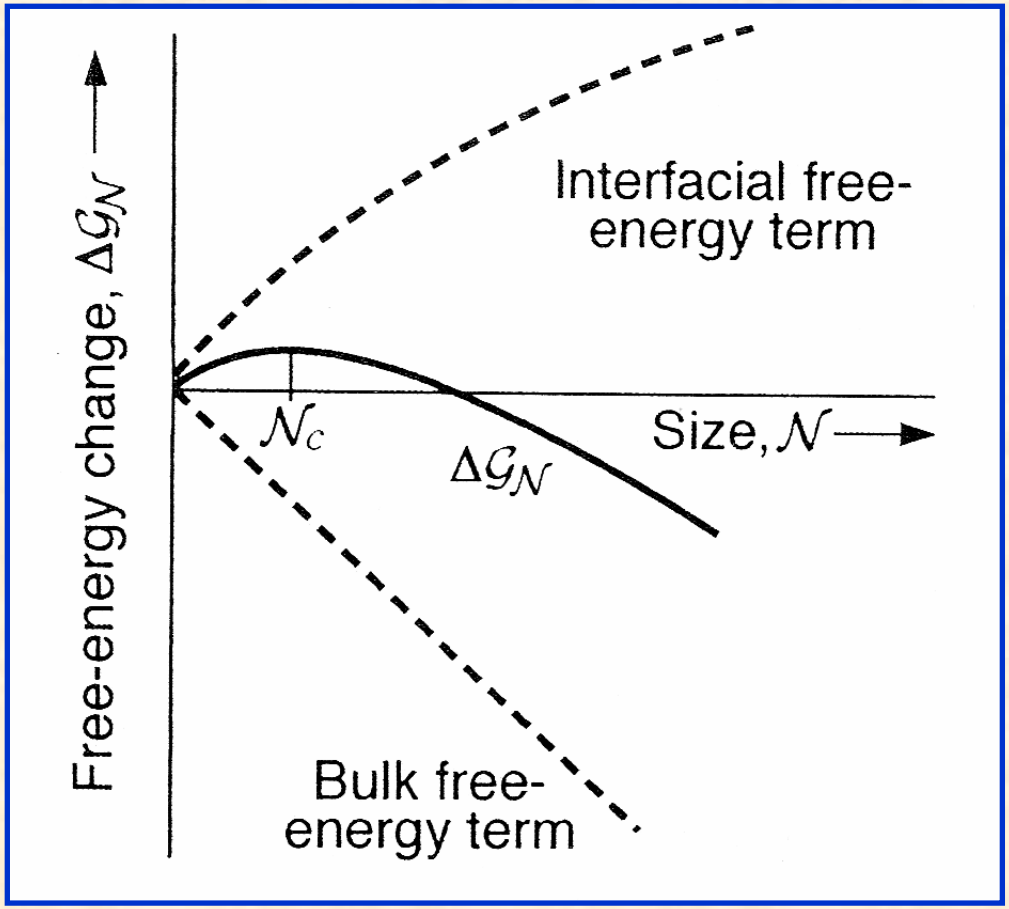


**Fahrenheit (1724)**

**Volmer & Weber (1926)**

**Turnbull (1952)**

**The general model of nucleation is well studied and well understood: with a driving potential $|\Delta_{rxn}G| > 0$ and sufficient thermal energy, transformations will occur at rates that can be predicted.**

***But does the magnitude of $\Delta_{rxn}G$ have an effect?***

**General expectation for silicate glass-ceramics: liquidus phase forms**

BROWN

# Big $\Delta_{rxn}G$? Many, Many Possibilities! Kinetic Path is Key

**With a very small $\Delta_{rxn}G$, one reaction is possible: the equilibrium one shown on the phase diagram**

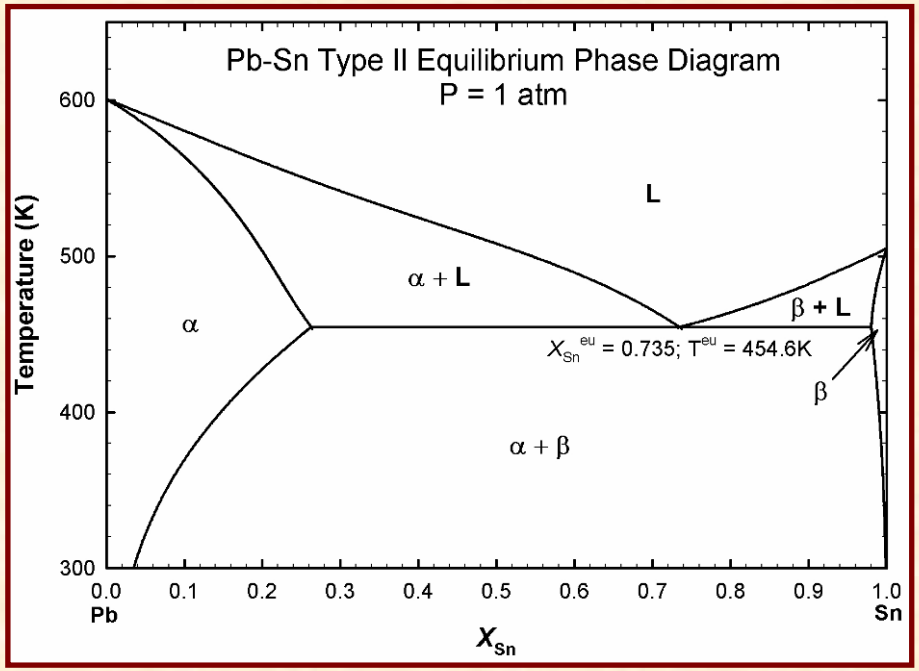


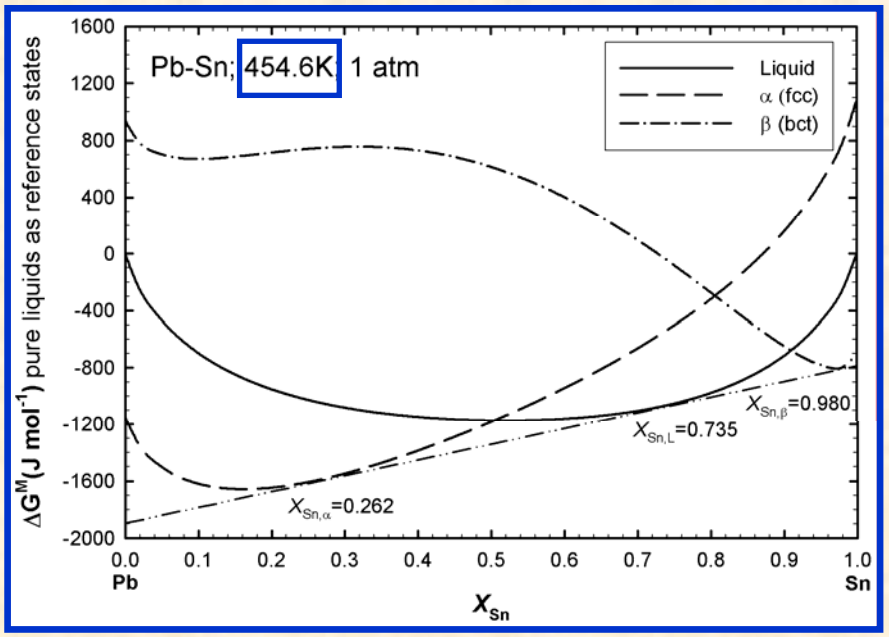


**With a large $\Delta_{rxn}G$, many reactions are possible (shown for $X^{eu}$ liquid): kinetics often dictates what is seen, not (necessarily) equilibrium thermodynamics.**

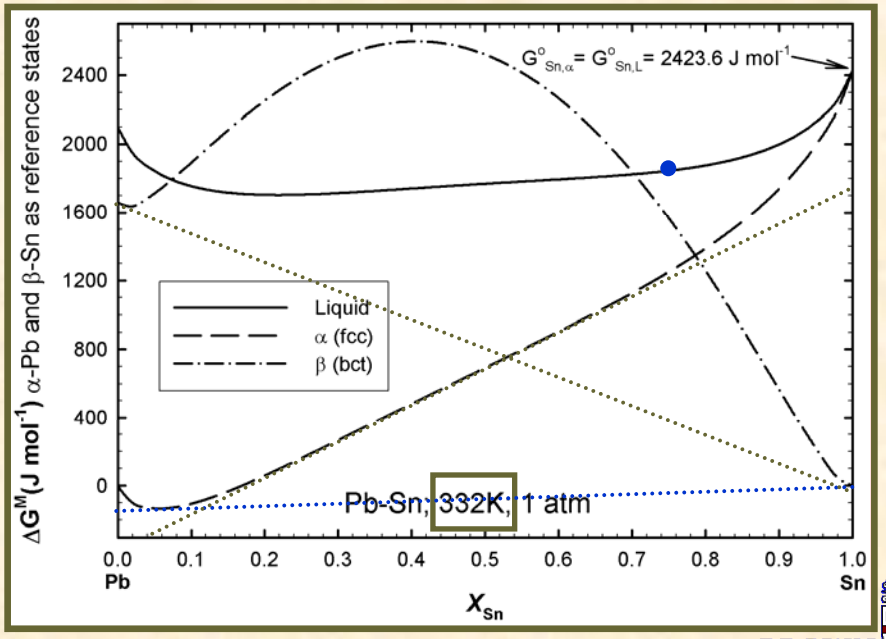


BROWN

# Eg.: Large Undercooling in MgO-$SiO_2$: Forsterite Glass-Ceramics

**Hypoeutectic melt composition experiences both metastable liquid-phase immiscibility and nucleation of metastable $Mg_2SiO_4$**

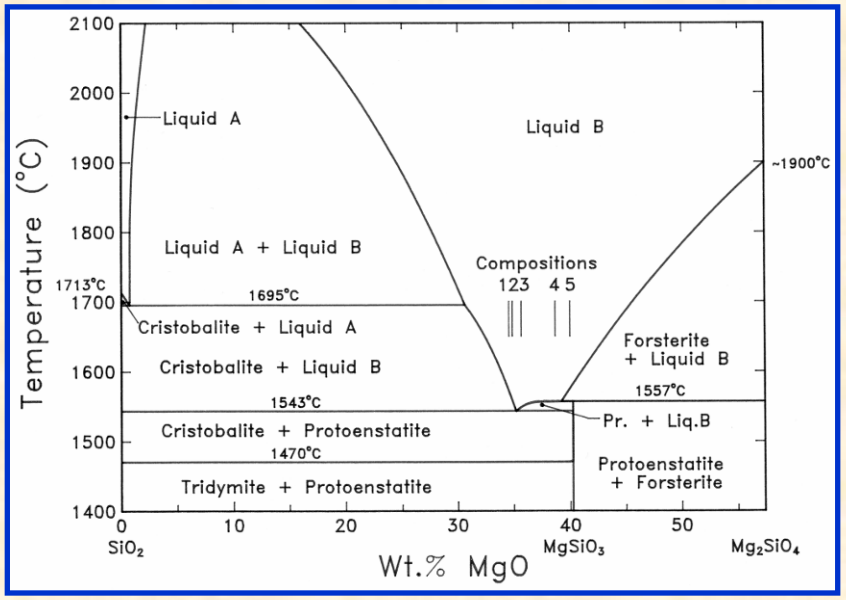


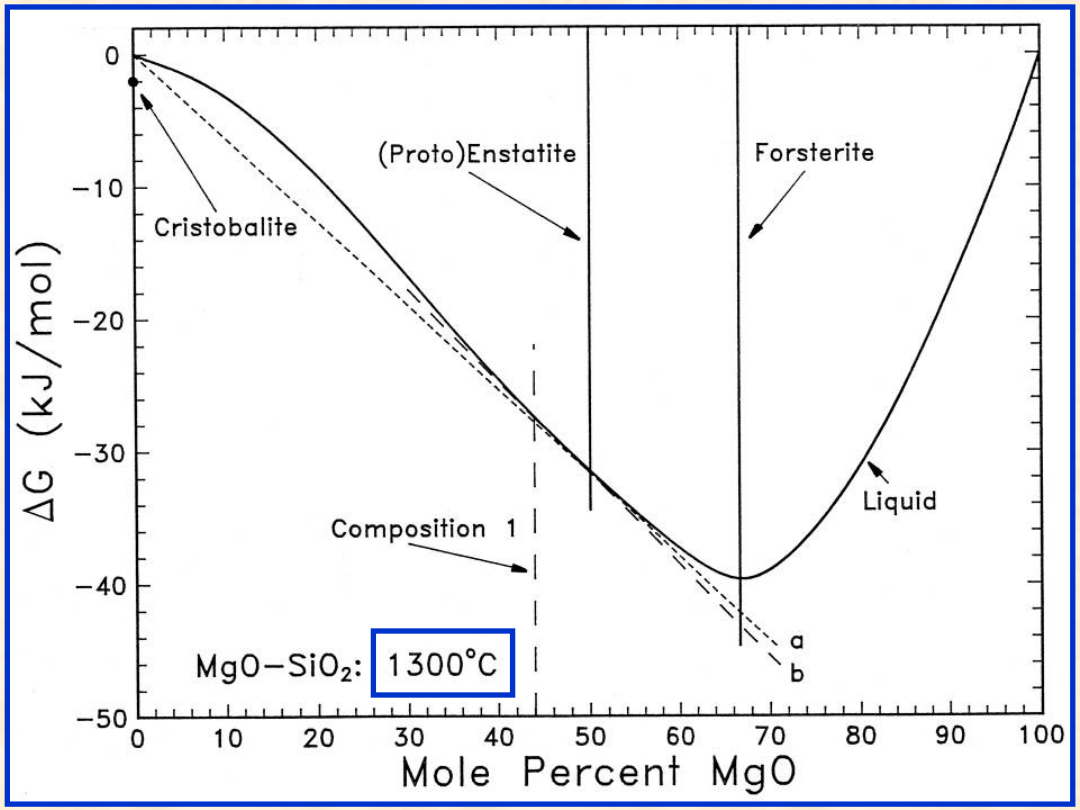


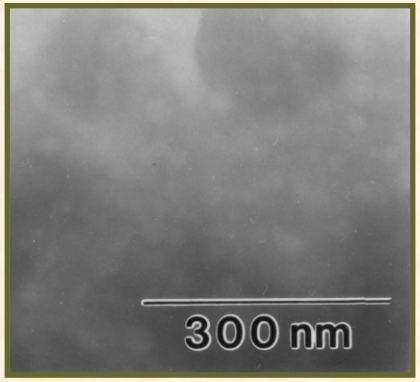


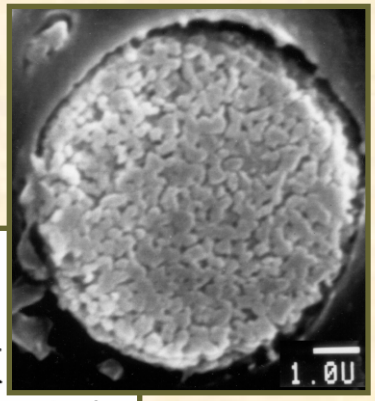


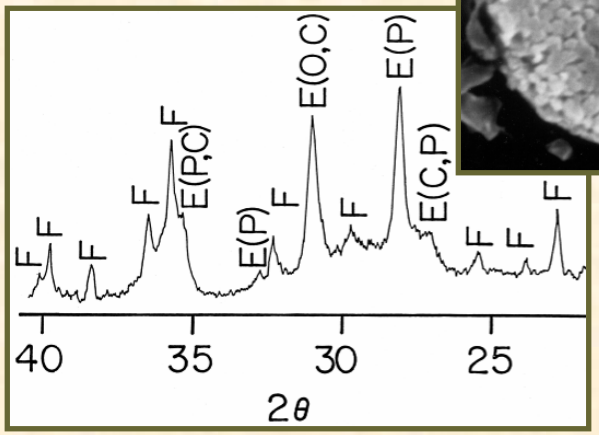


BROWN

# Thermodynamic Landscape and Prigogine's Bifurcations

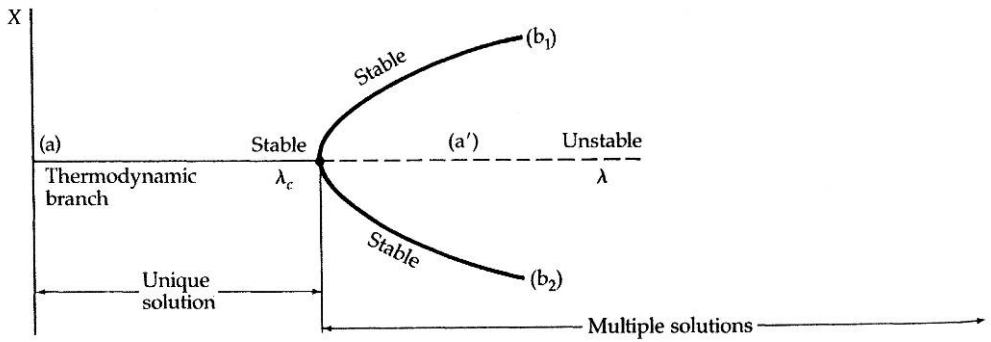


***Figure 30*** Bifurcation diagram showing how a state variable $X$ is affected when the control parameter $\lambda$ varies. A unique solution *(a)*, the thermodynamic branch, loses its stability at $\lambda_c$. At this value of the control parameter new branches of solutions ($b_1$, $b_2$), which are stable in the example shown, are generated.

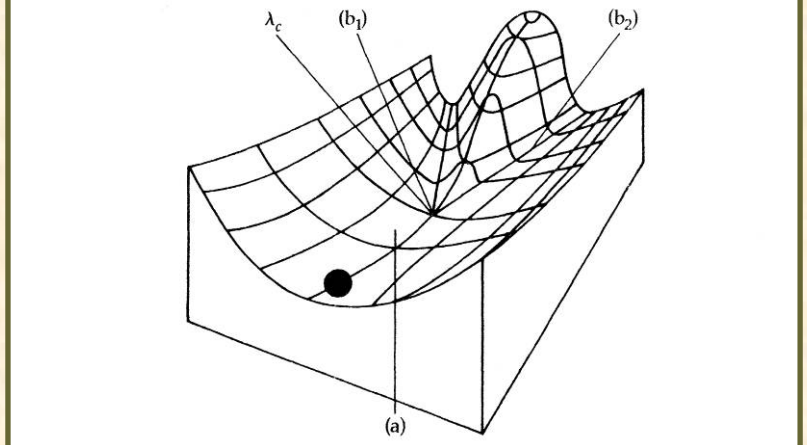


***Figure 31*** Mechanical illustration of the phenomenon of bifurcation.

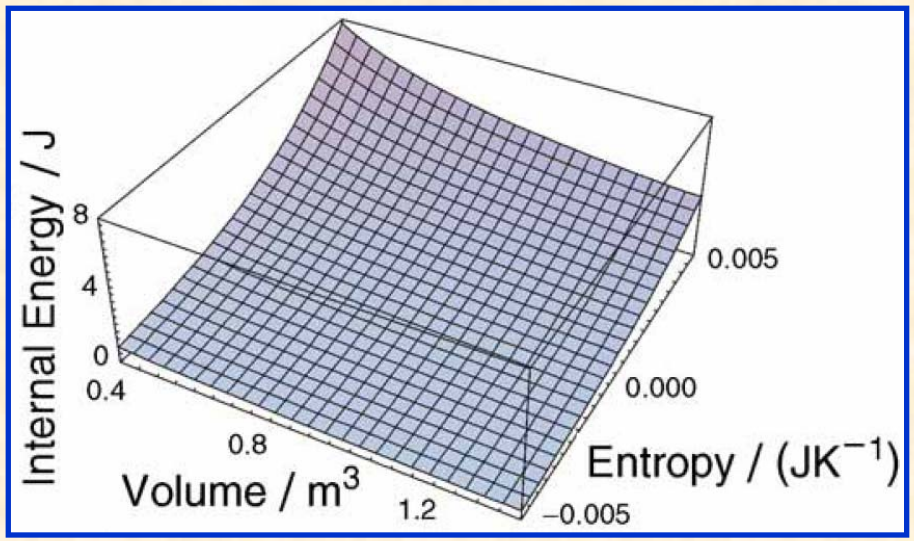


**Thermodynamic (landscape) branch for an ideal gas—PV = RT**

**Small perturbations from equilibrium can be easily understood and analyzed: the system is constrained to the "thermodynamic branch."** ***But what of large perturbations?***

BROWN

# Thermodynamic Landscape and Prigogine's Bifurcations

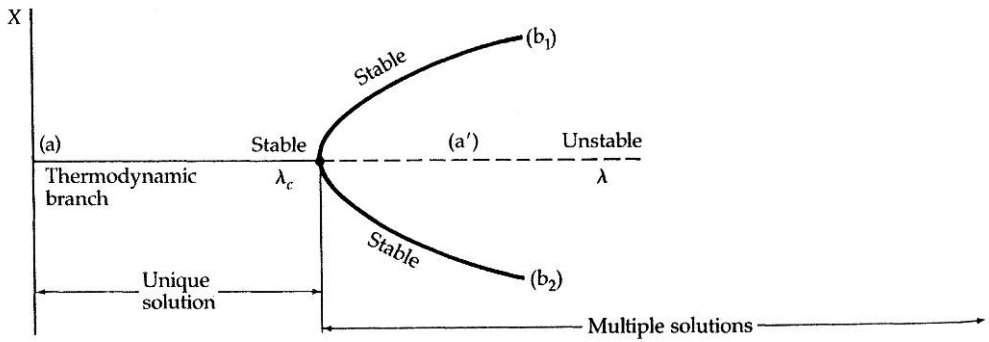


***Figure 30*** Bifurcation diagram showing how a state variable X is affected when the control parameter $\lambda$ varies. A unique solution *(a)*, the thermodynamic branch, loses its stability at $\lambda_c$. At this value of the control parameter new branches of solutions ($b_1$, $b_2$), which are stable in the example shown, are generated.

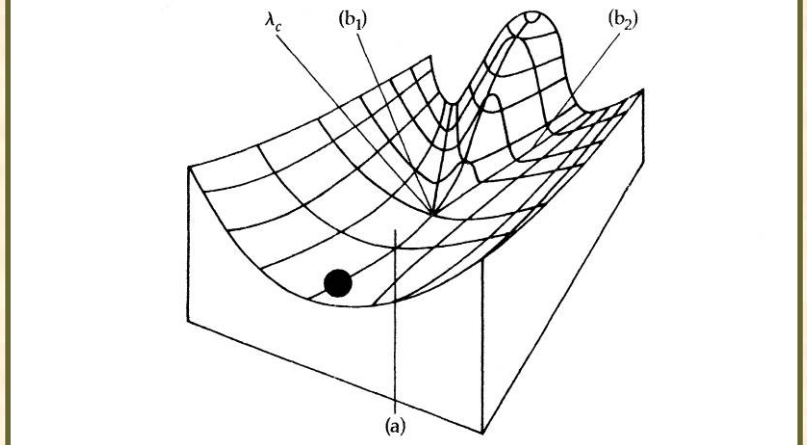


***Figure 31*** Mechanical illustration of the phenomenon of bifurcation.

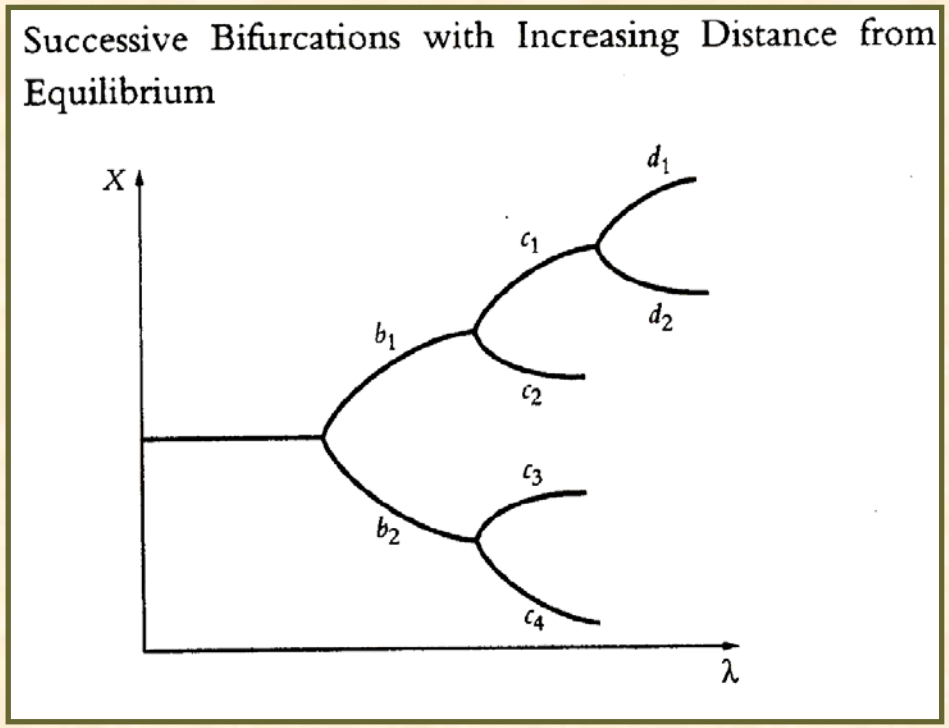


**Pushing the system beyond a certain state opens up a variety of possibilities—*branches of metastability*.**

**1. The branch that is accessed is a function of kinetics.**

**2. Branches can produce *order*, with potential *persistence.***

**The old future's gone…**

**—John Gorka**

BROWN

# Cation Roles: Network Former or Network Modifier

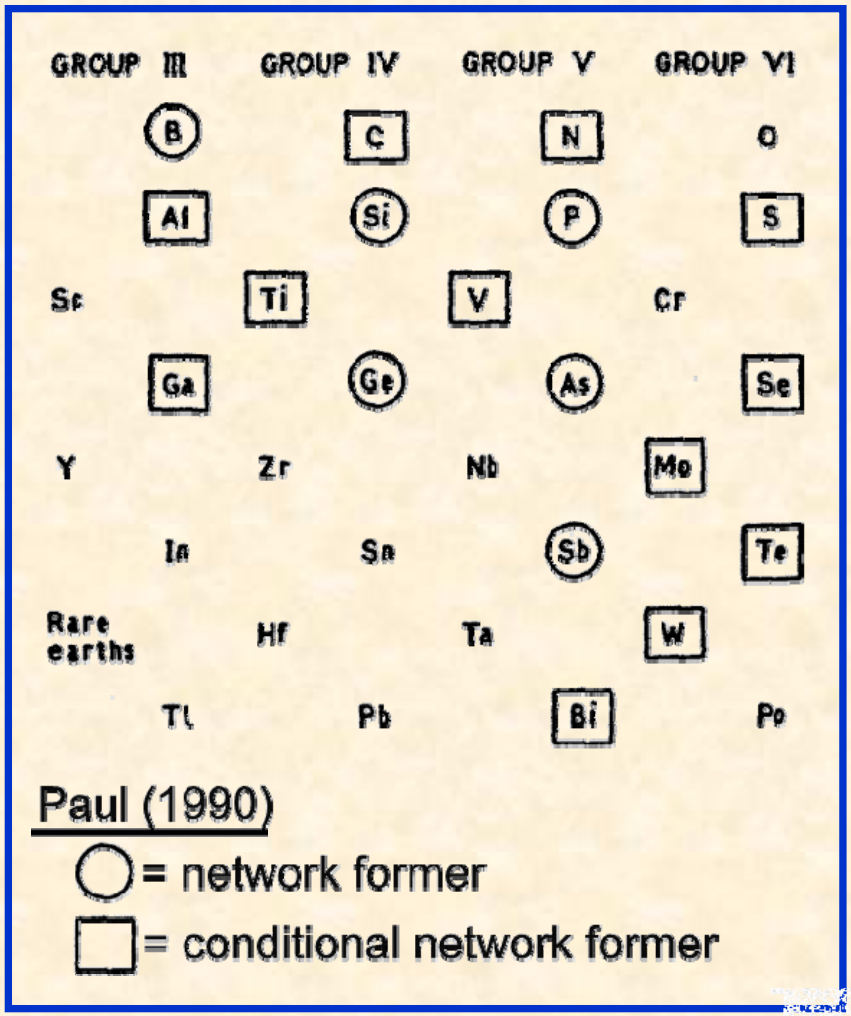


## Structural Role of Iron Cations in Aluminosilicate Melts/Glasses

$Fe^{2+}$ -- network modifier

$Fe^{3+}$ -- network modifier:

$Fe^{3+}:Fe^{2+} < 1:2$

-- mixed modifier/former:

$1:2 \leq Fe^{3+}:Fe^{2+} \leq 1:1$

-- network former:

$Fe^{3+}:Fe^{2+} > 1:1$

→ *Alkali cations act more aggressively to stabilize $Fe^{3+}$ as a network former than do alkaline earth cations*

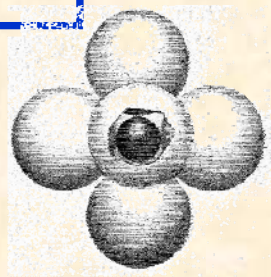

$\frac{r_{Fe^{2+}}}{r_{O^{2-}}} = 0.53$

$\Rightarrow CN = VI$

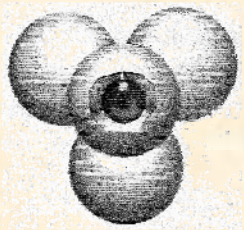

$\frac{r_{Fe^{3+}}}{r_{O^{2-}}} = 0.45$

$\Rightarrow CN = IV\,?$

BROWN

# Oxidation State and Liquidus Surface

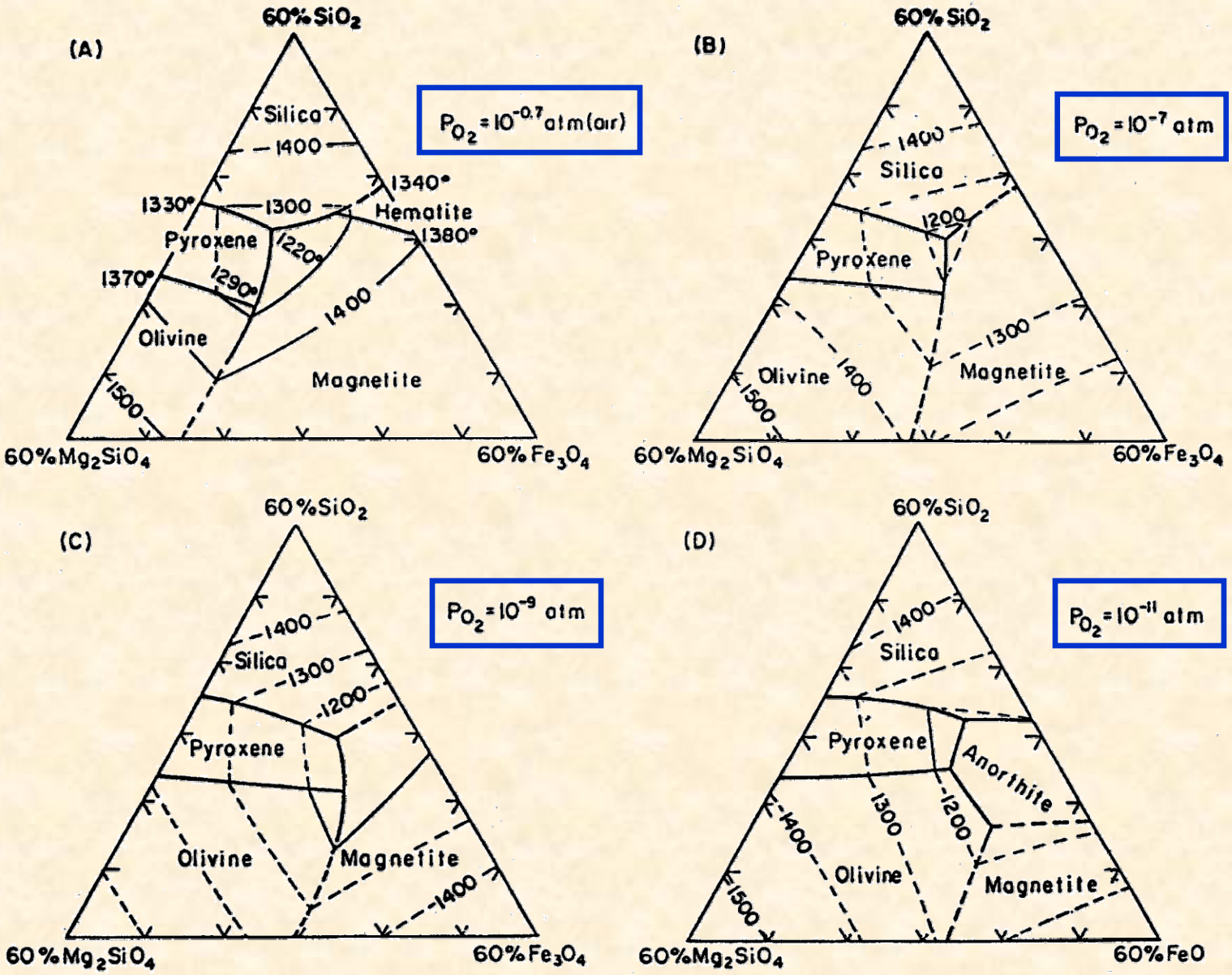


Roeder & Osborn, Am. J. Sci., 264 (1966): M-F-S @ 40 wt% $CaAl_2Si_2O_8$

BROWN

# Redox Dynamics in Silicate Melts: Chemical Diffusion of an Oxygen Species?

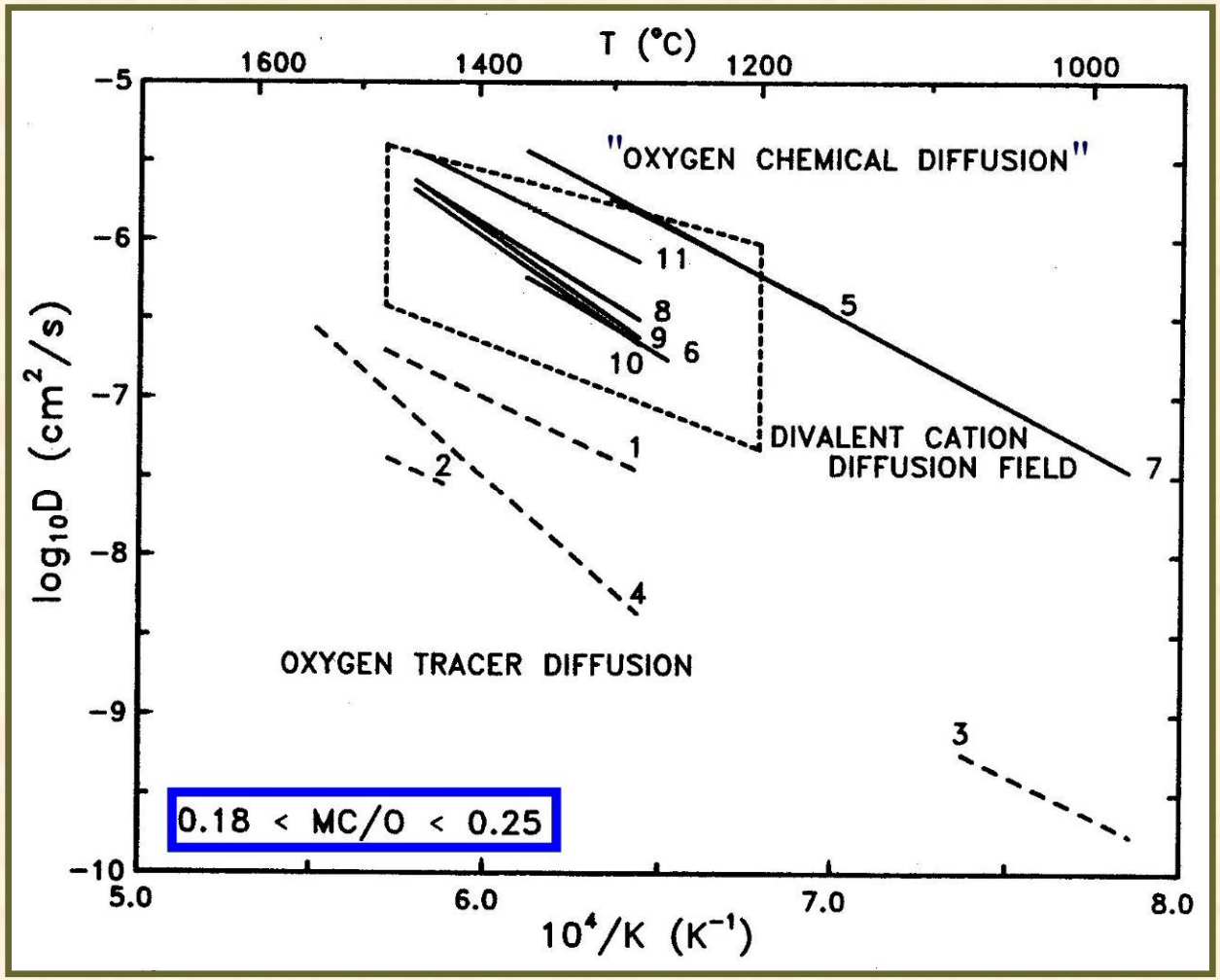


1 & 2: Dunn (1982)

3: Yinnon & Cooper (1980)

4: Muehlenbachs & Kushiro (1974)

5 & 6: Wendlandt (1980)

7: Doremus (1960)

8-11: Dunn (1983)

Oxygen diffusion "remains one of the less well understood aspects of transport in silicate melts."

--S. Chakraborty, RiMG 32 (1995)

BROWN

# "Modes" of Dynamic Oxidation‡

**Given the Fick-Einstein Relationship:** $j_i = -\frac{c_i D_i}{RT}\frac{d\eta_i}{d\xi} = -\frac{c_i D_i}{RT}\left(\frac{d\mu_i}{d\xi} + z_i F\frac{d\varphi}{d\xi}\right)$

$Fe^{2+}$-bearing melt/glass

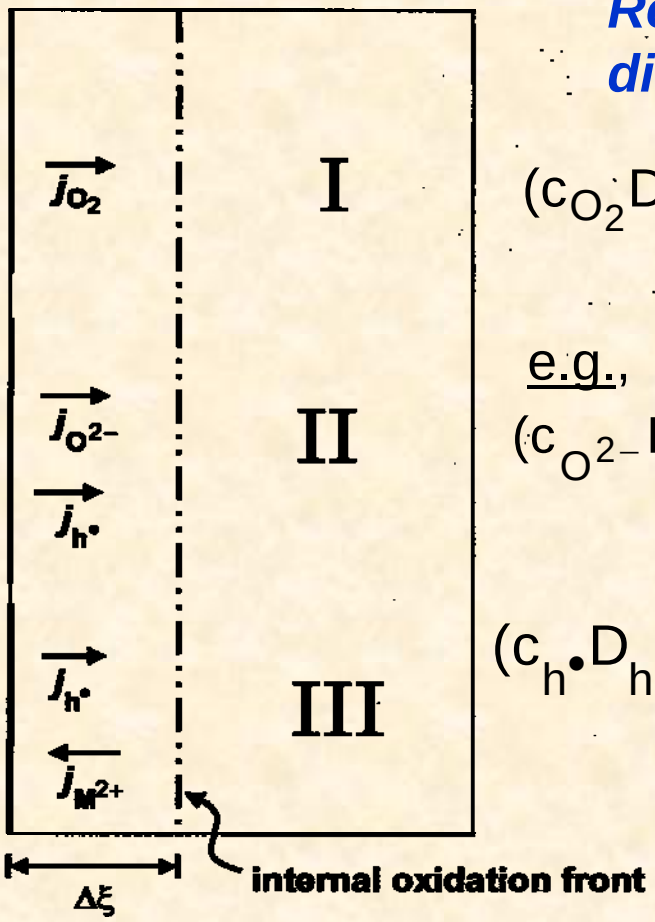


***Relative Transport Coefficients dictate the kinetic response!*** **E.g.:**

$(c_{O_2} D_{O_2})$ largest

e.g.,

$(c_{O^{2-}} D_{O^{2-}}) >> (c_{h^\bullet} D_{h^\bullet}) >> (c_{O_2} D_{O_2})$

→ *rate-limited by electronic conductivity*

$(c_{h^\bullet} D_{h^\bullet}) >> (c_{M^{2+}} D_{M^{2+}}) >>$

$[(c_{O^{2-}} D_{O^{2-}})$ or $(c_{O_2} D_{O_2})]$

→ *rate-limited by modifier-cation diffusion*

**independent (*parallel*) kinetic responses: "*different paths on the thermodynamic landscape*"**

‡anhydrous conditions

BROWN

# Melt Oxidation: "Isothermal Undercooling"

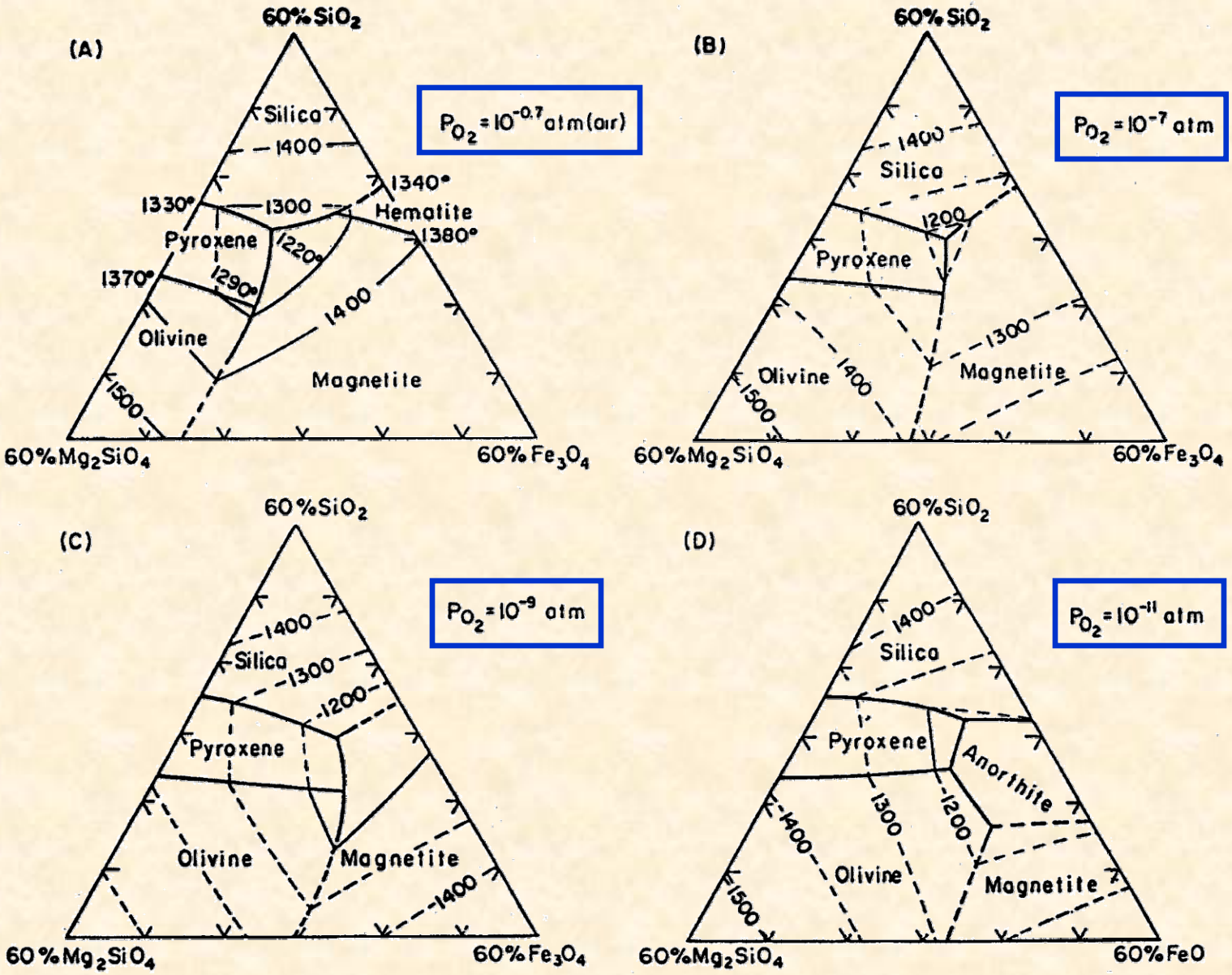


Roeder & Osborn, Am. J. Sci., 264 (1966): M-F-S @ 40 wt% $CaAl_2Si_2O_8$

BROWN

# Experimental Approach: AeroAcoustic Levitation (AAL)

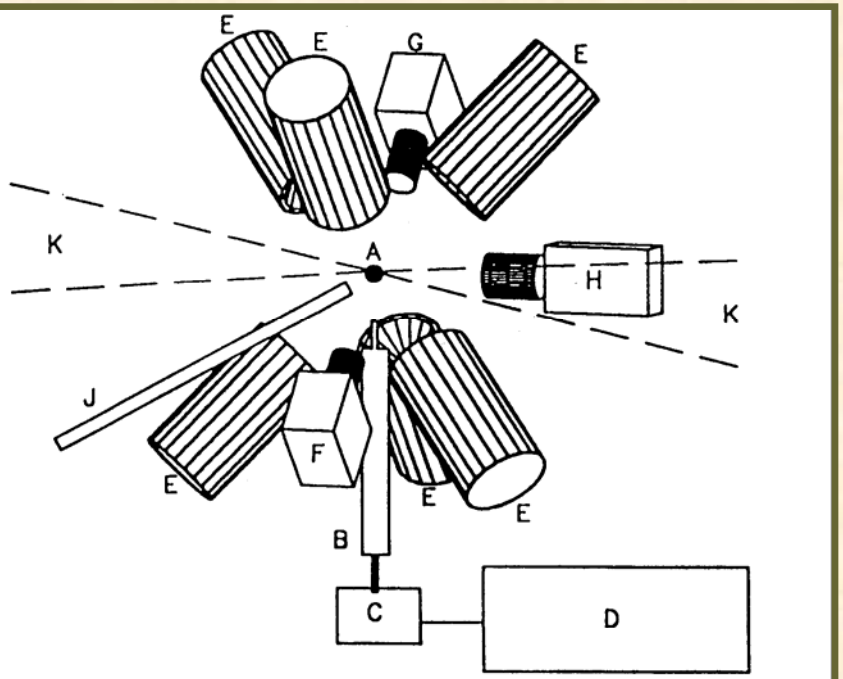


FIG. 1. Schematic of the aero-acoustic levitator. *A*, levitated specimen; *B*, gas flow tube and heater; *C*, translation stage; *D*, flow control system; *E*, acoustic transducers (three axis); *F*, diode laser specimen illuminator (3 axis); *G*, specimen position detector (3 axis); *H*, video camera; *J*, vacuum chuck; *K*, laser beam heating.

Weber et al., RSI, 65 (1994)

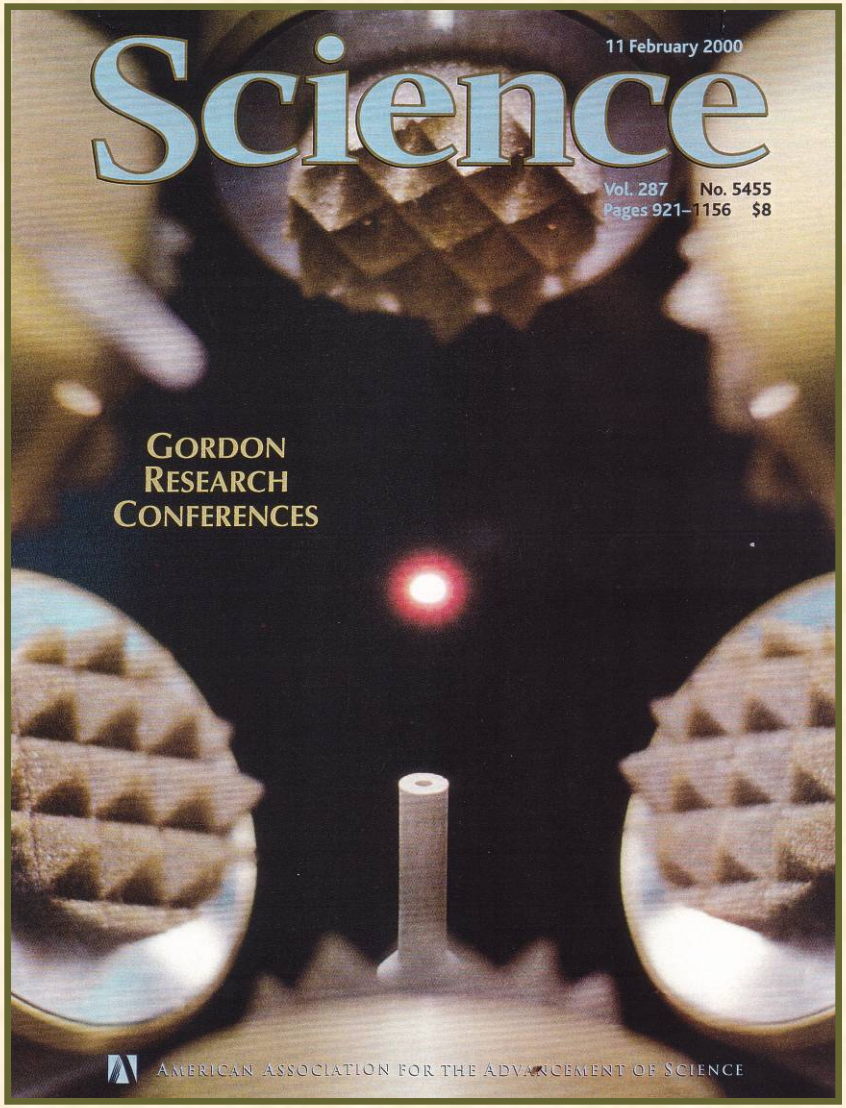


4 cm

BROWN

# Oxidation of Basalt Liquid

## *Columbia River Flood Basalt; Aero-Acoustic Levitation*

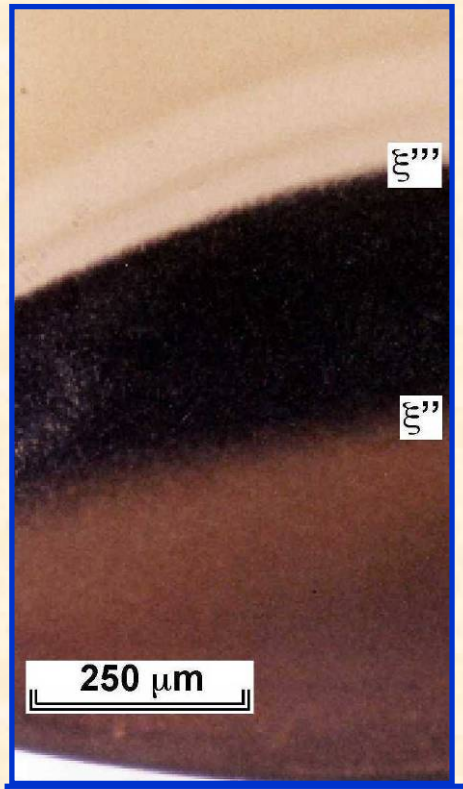


**1400°C**

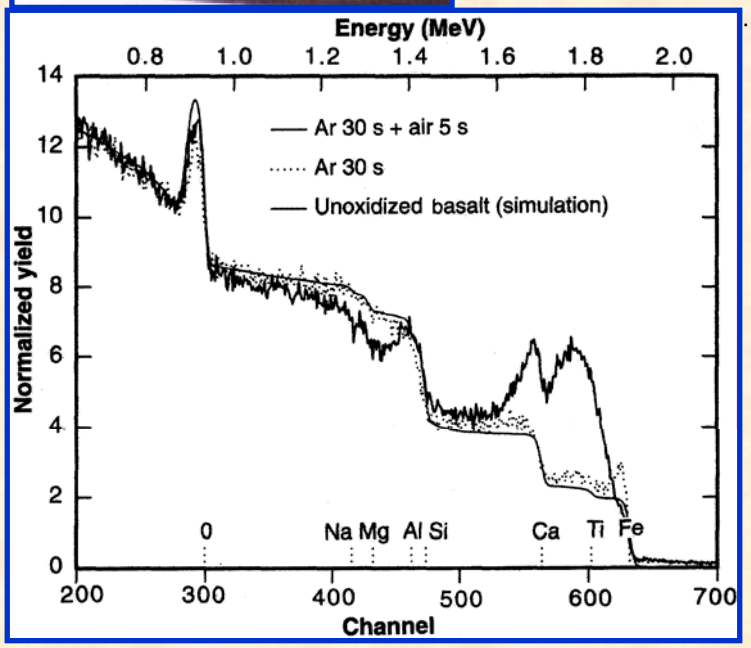


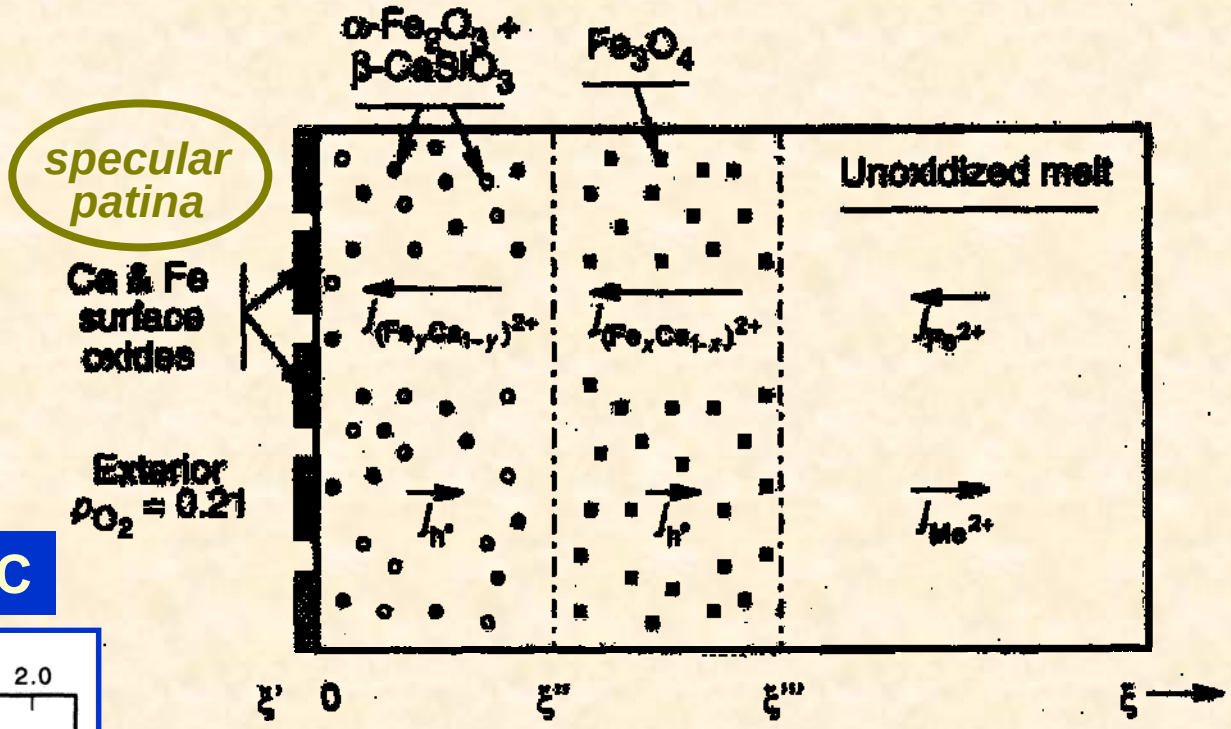


- **Oxidation in Ar(g) ($a_{O2}$~$10^{-6}$) mobilizes $Fe^{2+}$, which diffuses to the free surface**
- **Oxidation in air ($a_{O2}$=0.21) mobilizes both $Fe^{2+}$ and $Ca^{2+}$**

→ ***data are <u>unequivocal</u> proof that oxidation is accomplished & rate-limited by chemical diffusion of divalent network modifier cations!***

BROWN

# Basaltic Glass near $T_g$: $Fe^{3+}$ Stabilized as Network Former

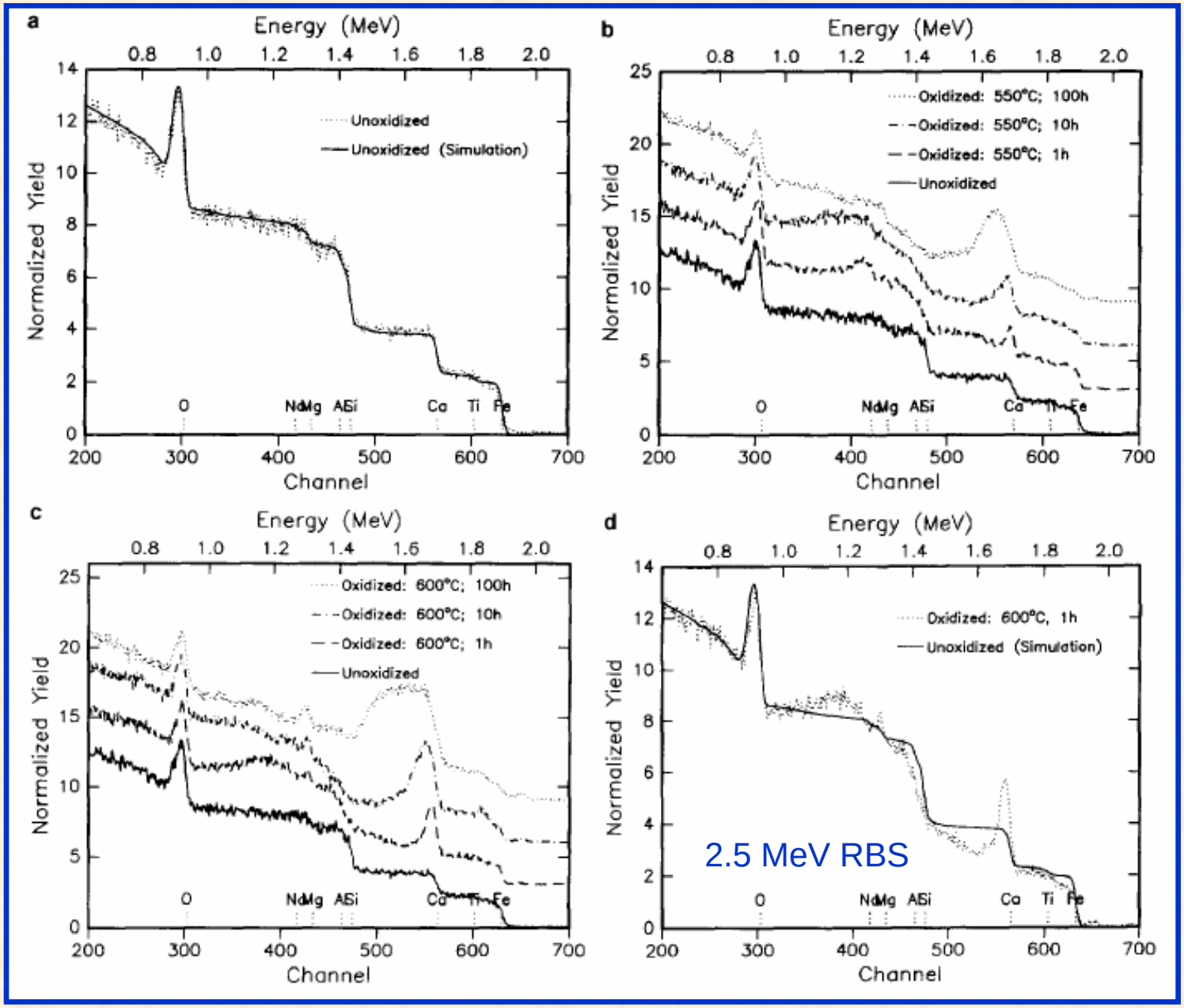


- **Surface: discontinuous ppts of lime & periclase (+minor nepheline)**
- **$Na^+$ from depth stabilizes $Fe^{3+}$ as network former: *no ferrite formation!***

BROWN

# Polymerization Model of Paul Hess (1980) applied to oxidation

(cf. Schaeffer, 1984; Kress & Carmichael, 1991)

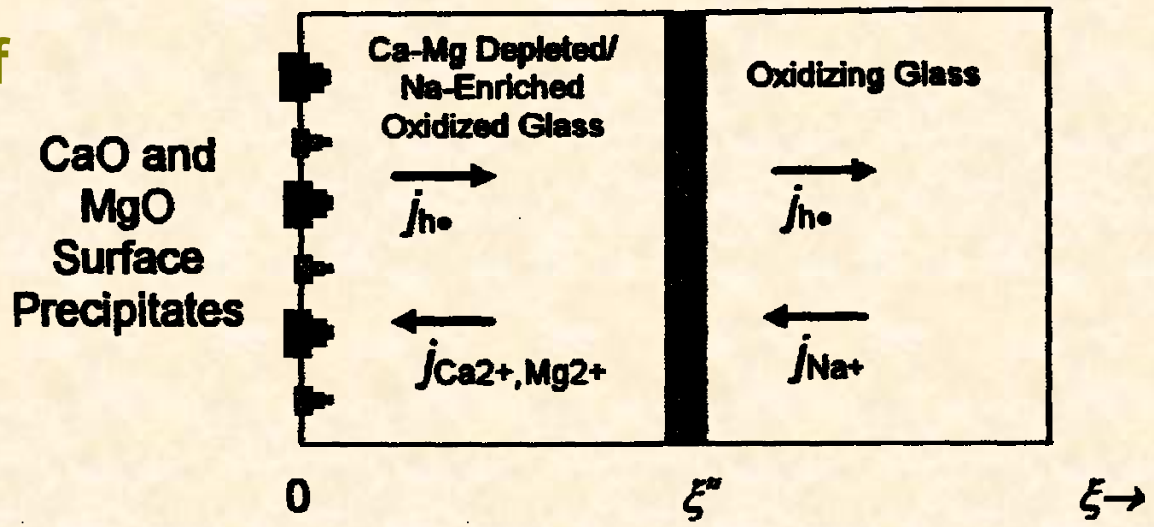


**Reactions:**

at $\xi = 0$:

$$\tfrac{1}{2}O_2(g) + 4SiOFe_{0.5} + 2SiO(\overleftarrow{Ca_eMg_f})_{0.5} \rightarrow 6\overrightarrow{SiOFe_{0.33}} + eCaO + fMgO$$

at $\xi = \xi''$:

$$6\overrightarrow{SiOFe_{0.33}} + x\overleftarrow{SiONa} + 4SiO(Ca_aMg_b)_{0.5} \rightarrow (2-x)NaFeO_2 + (2x-2)SiONa$$

$$+3x\overrightarrow{SiOFe_{0.33}} + (4-2x)SiOSi$$

$$+2SiO(Ca_cMg_d)_{0.5} + 2SiO(\overleftarrow{Ca_eMg_f})_{0.5}$$

***Oxidation of a basalt glass near $T_g$***

where

$3SiOFe_{0.33} \equiv h^{\bullet}$; $2SiO(Ca,Mg)_{0.5} \equiv (Ca,Mg)^{2+}$; $SiONa \equiv Na^{+}$;

$2SiOFe_{0.5} \equiv Fe^{2+}$; $NaFeO_2 \equiv$ network-forming $Fe^{3+}$

BROWN

# Dynamic Reduction: The Mirror Image?

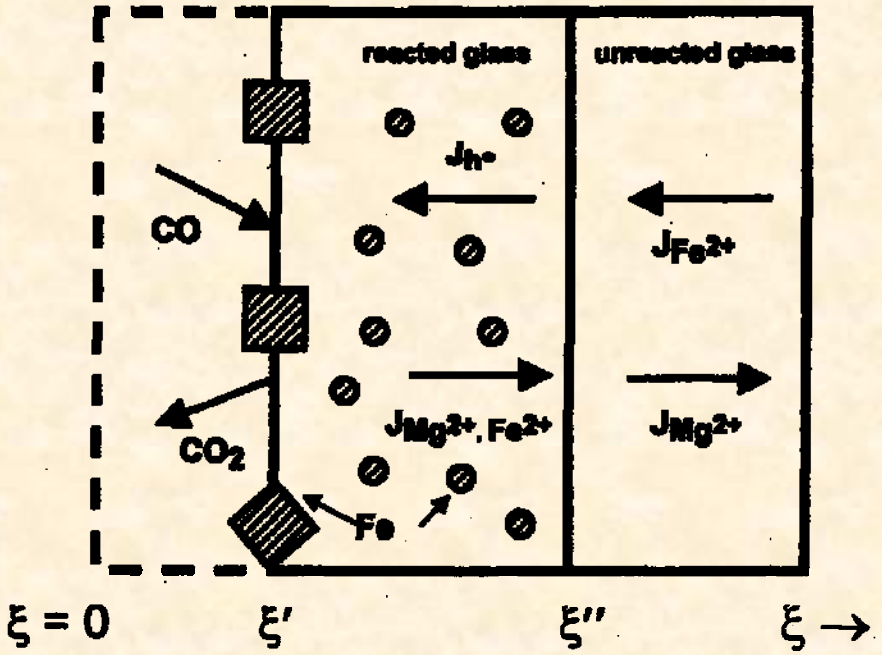


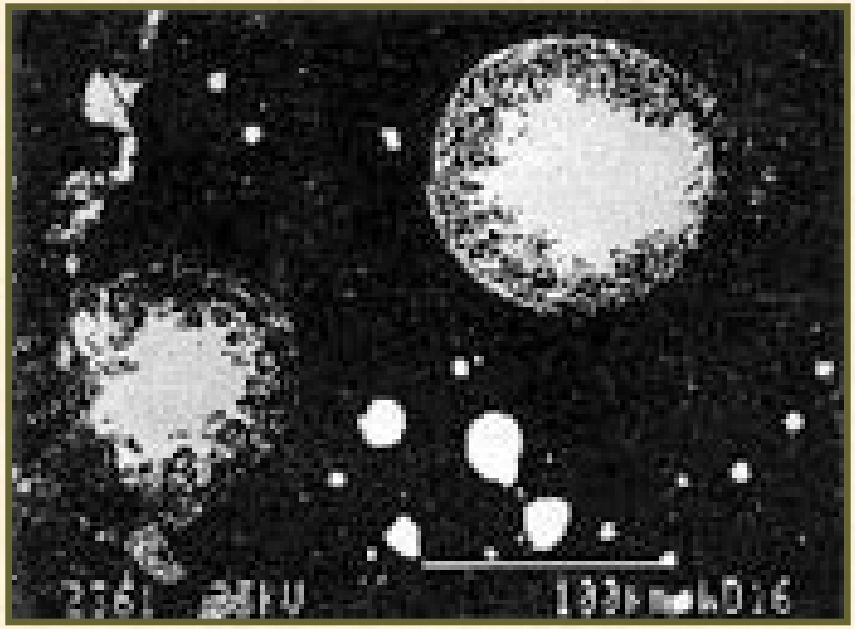

Semarkona LL3.0; Bourot-Denise *et al.* (2001)

*Mechanism:*

Oxygen ablates (chemically) from free surface; creates excess cations, which diffuse inwards and are charge-compensated by outward motion of $h^\bullet$.

*Motivation:*

Thermokinetics responsible for distribution (concentric, periodic precipitation) of metal in primitive chondrules

BROWN

## Original Melt Compositions

| | FeMAS | | | FeCMAS | |
|---|---|---|---|---|---|
| Oxide | wt% | mol% | | wt% | mol% |
| $SiO_2$ | 59.2 | 59.2 | | 59.2 | 63.3 |
| $Al_2O_3$ | 15.5 | 9.1 | | 13.0 | 8.2 |
| $Fe_2O_3$ | 2.1 | 0.8 | | 5.5 | 2.2 |
| FeO | 5.6 | 4.7 | | 7.5 | 6.7 |
| MgO | 17.4 | 25.9 | | 6.0 | 9.6 |
| CaO | 0.1 | 0.1 | | 8.8 | 10.1 |
| $Fe^{2+}/Fe_{total}$ | 0.75 | | | 0.60 | |
| NBO/T | 0.53 | | | 0.38 | |
| MC/O | 0.18 | | | 0.17 | |

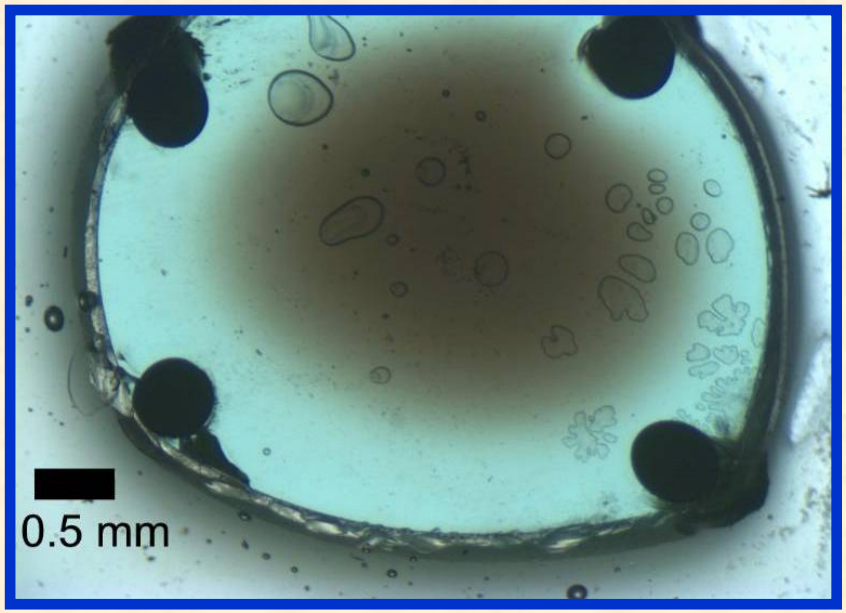


*FeMAS; 1400°C; 0.5h; QIF–2*

## Experimental Approach

- Original material: bulk oxide glasses prepared conventionally (Fe-soaked Pt crucibles); initial $a_{O2}$ ~ FMQ
- Reaction Vessel: vertical tube furnace; $MoSi_2$ resistance elements; alumina muffle
- 2–3mm cube sectioned; suspended in wire cage (Fe, Mo, Pt)
- Temperature range: 1350-1450°C (*>silicate melt liquidus;* < $T_{m,Fe}$)
- Dynamic gas mixing $CO:CO_2$ in range 240:1 (QIF–2) to 1750:1 (QIF–4); 200 $cm^3min^{-1}$
- Active measurement of $a_{O2}$ (YSZ sensor)
- Free-fall quench

BROWN

# Fe-MAS Reduction Results: Kinetics

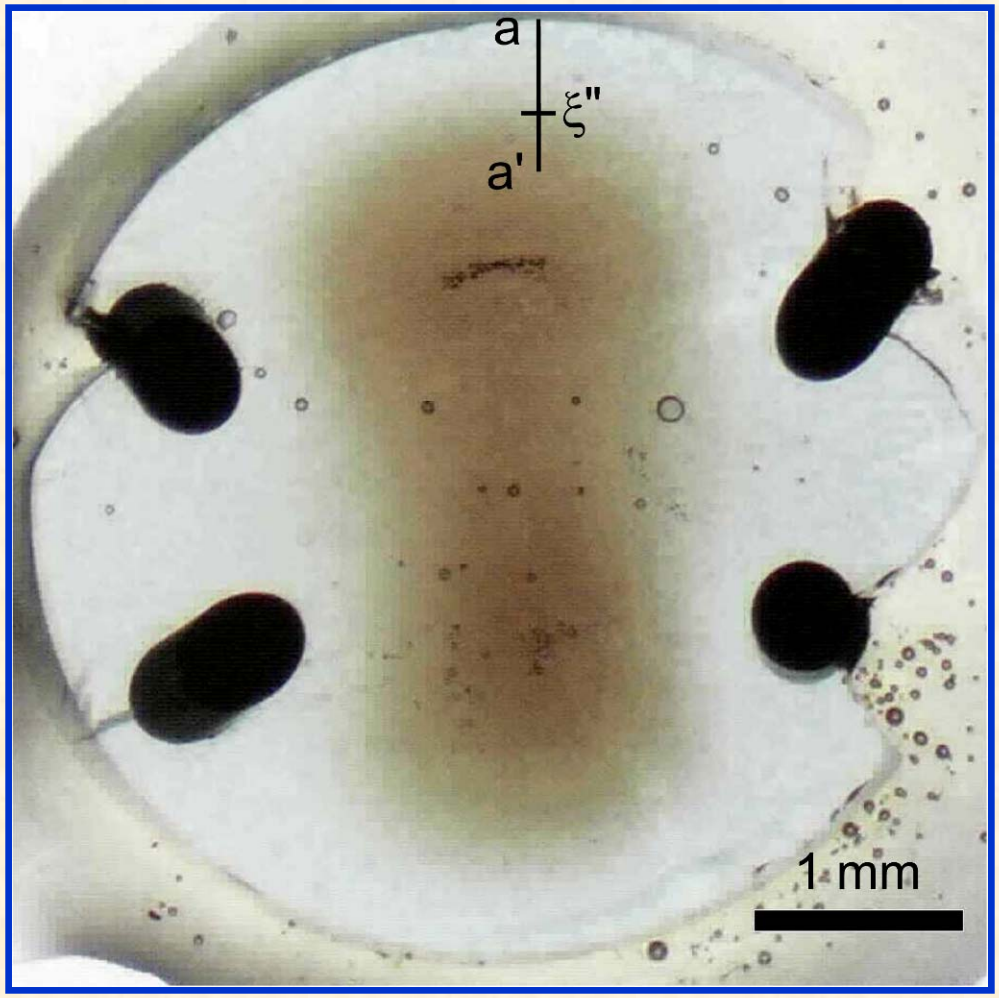


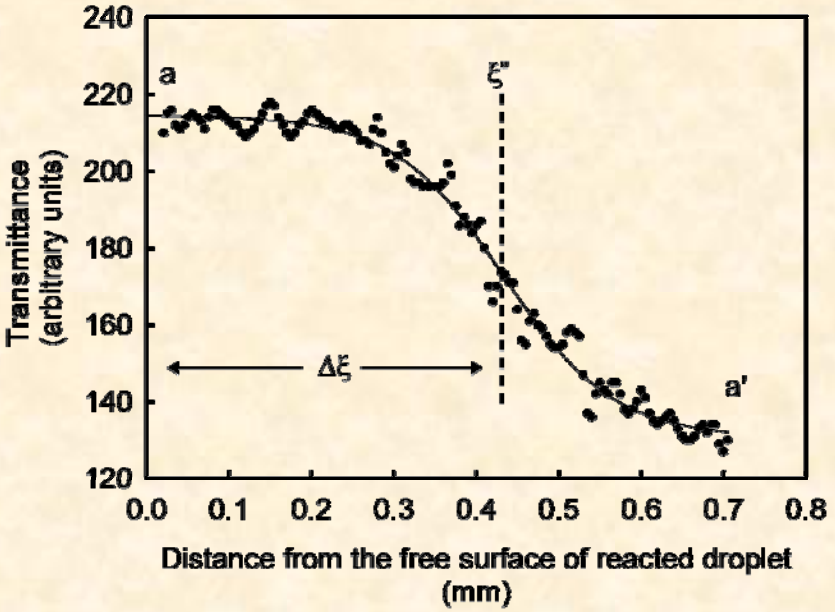


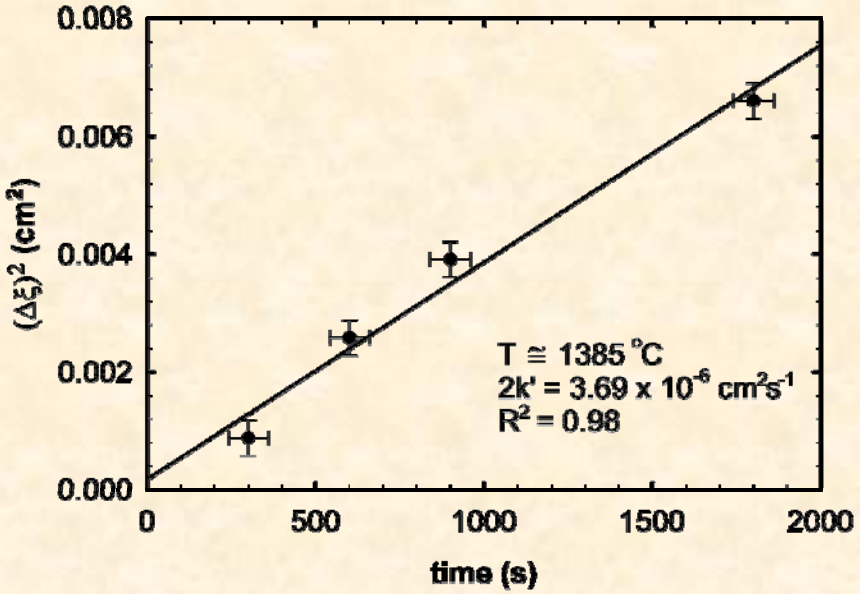


**T = 1380°C; $p_{O2} \approx 10^{-13}$ atm; t = 0.5 h**

BROWN

# Fe-MAS Reduction Results: Microstructures

## Free Surface

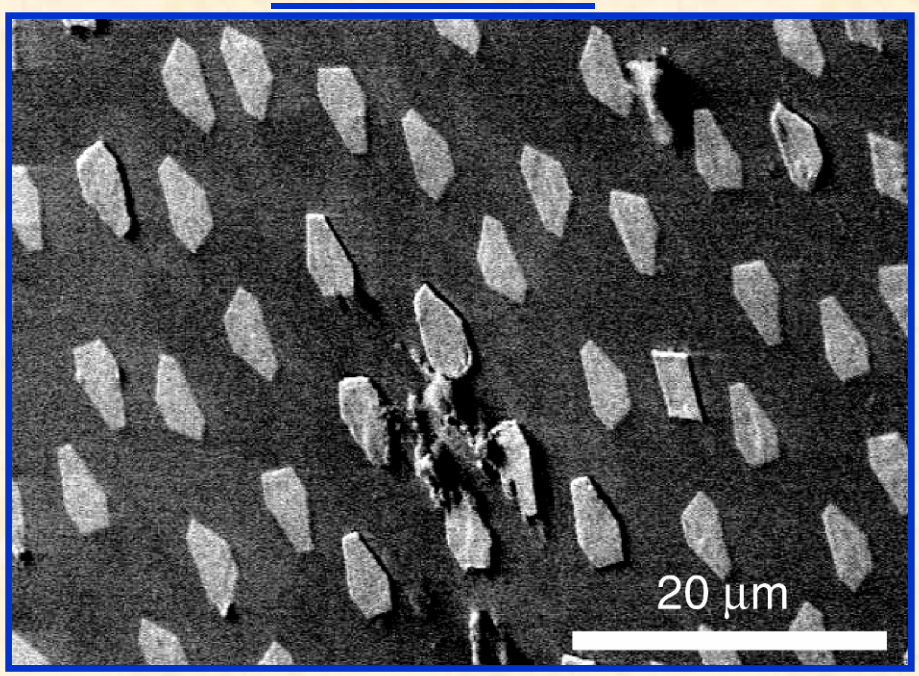


- Secondary Electron Image
- T = 1380°C; $p_{O2} \approx 10^{-13}$ atm; t = 1.0 h
- Pure bcc-Fe crystals: most demonstrating (111) with truncations being traces of {100}
- Vapor-phase transport important in coarsening

## Internal: ξ= ξ' to ξ''

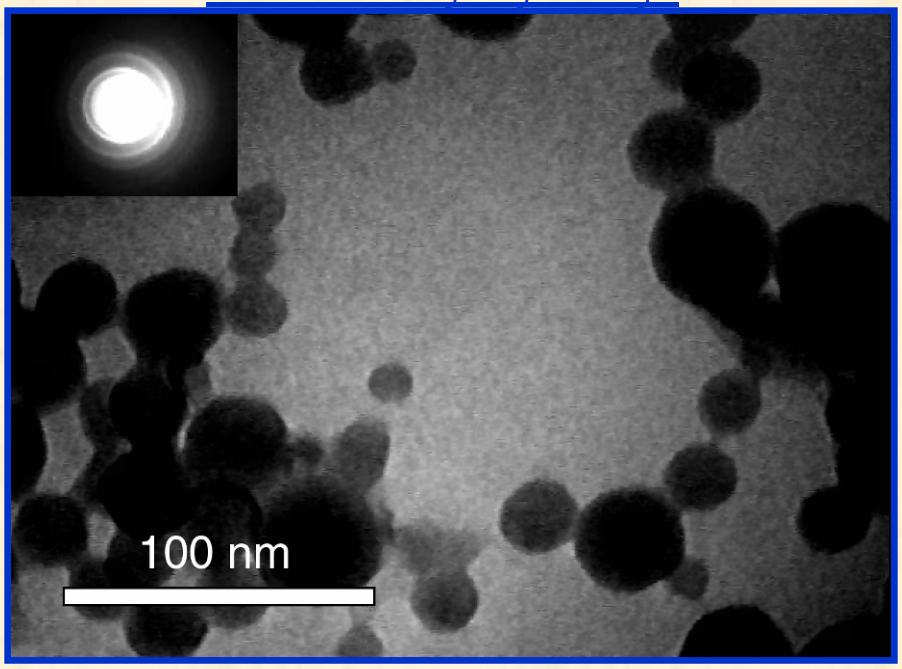


- T = 1380°C; $p_{O2} \approx 10^{-13}$ atm; t = 1.0 h
- Zero-loss (scattering contrast) image: dark phase is Fe°; HEED: bcc-Fe
- Size distribution is relatively uniform
- "String-of-pearls" morphology consistent with Modified Random Network (MRN) model for unreacted melt.

BROWN

# Reduction Kinetics: Polymerization Model following *Hess (1980)*

→ *Diffusion-limited reaction*

→ *Rate matching that of tracer diffusion of small divalent network modifier*

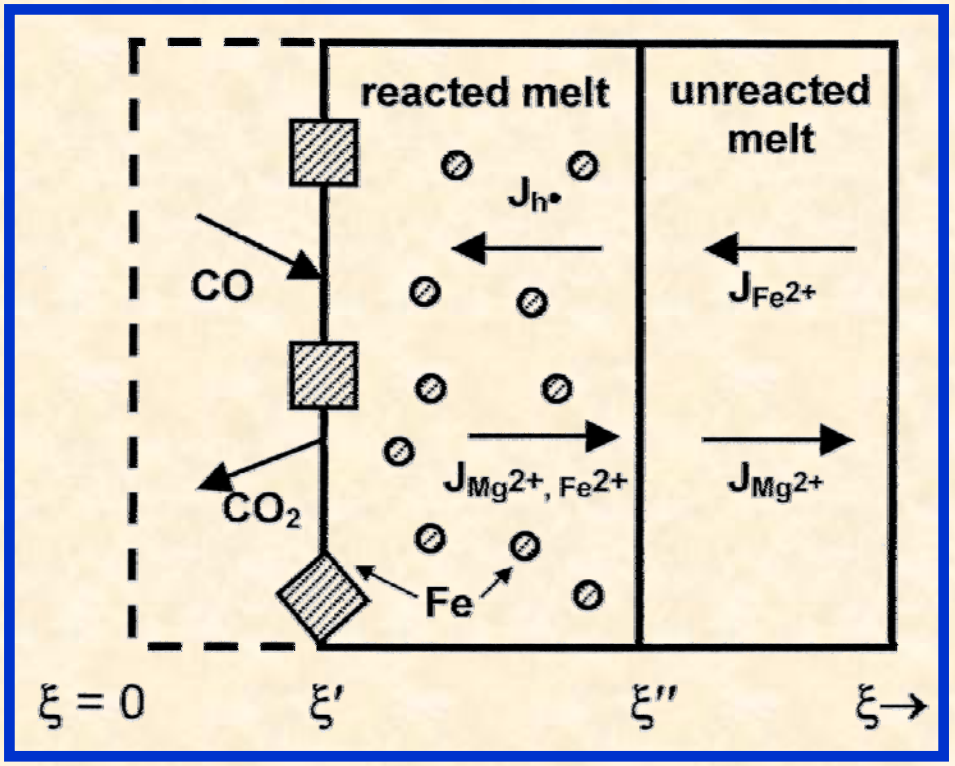


- **Reaction at Free Surface, ξ′:**

$$2SiOMg_{0.5} + 6SiOFe_{0.33} = MgO + 2SiOSi + 4SiOFe_{0.5} + \tfrac{1}{2}O_2(g)$$

$$= 2SiOMg_{0.5} + 4SiOFe_{0.5} + SiOSi + \tfrac{1}{2}O_2(g)$$

(*polymerization decreases*: MC/O goes from 3/8 to 3/7)

$3SiOFe_{0.33} \equiv h^\bullet$
$2SiOMg_{0.5} \equiv Mg^{2+}$

- **Reaction at Internal Reduction Front, ξ″:**

$$2SiOMg_{0.5} + 6SiOFe_{0.5} = Fe^{o} + 6SiOFe_{0.33} + 2SiOMg_{0.5}$$

(*polymerization increases*: MC/O goes from 4/8 to 3/8)

BROWN

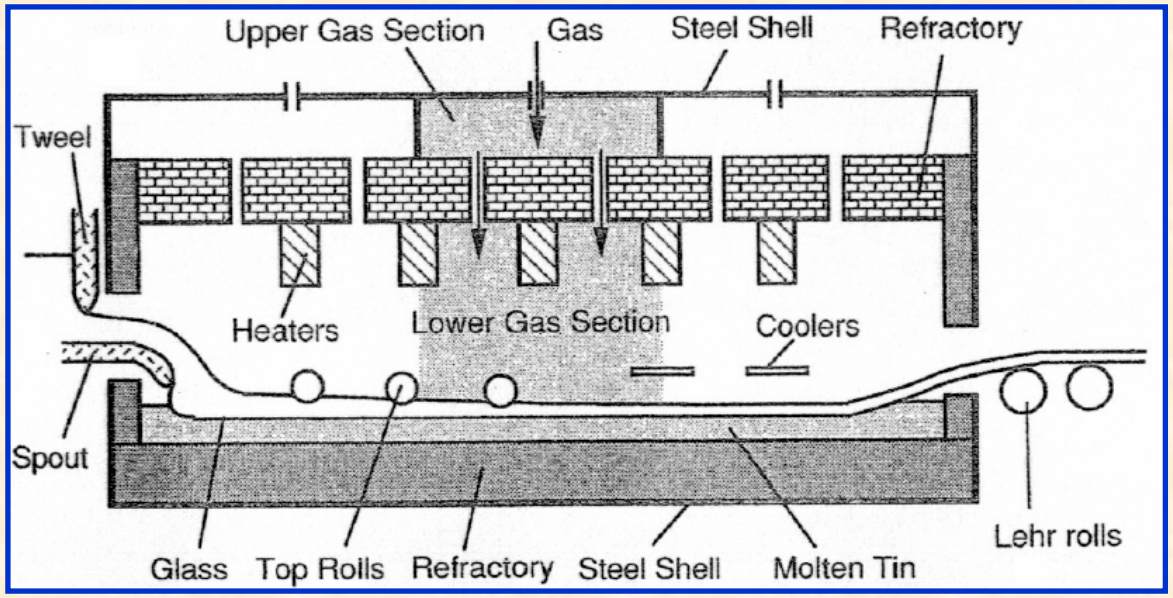


# Liquid Metal-Silicate Reactions: Spatial Control of Melt Structure

**NCS Melt on Liquid Sn°**

$1100 \geq T(^{o}C) \geq 600$

$1.5 \leq t\ (min) \leq 15$

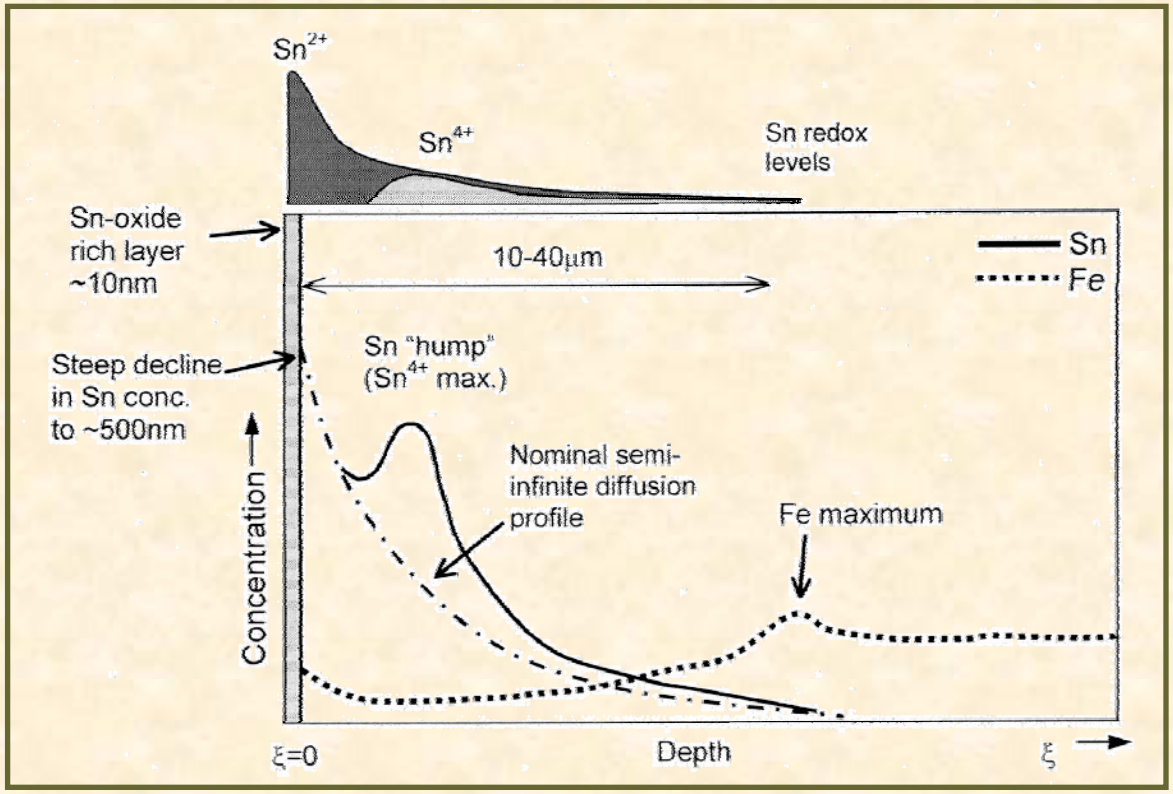


← Reaction Morphology

BROWN

# Experimental Apparatus and Specimen Assembly

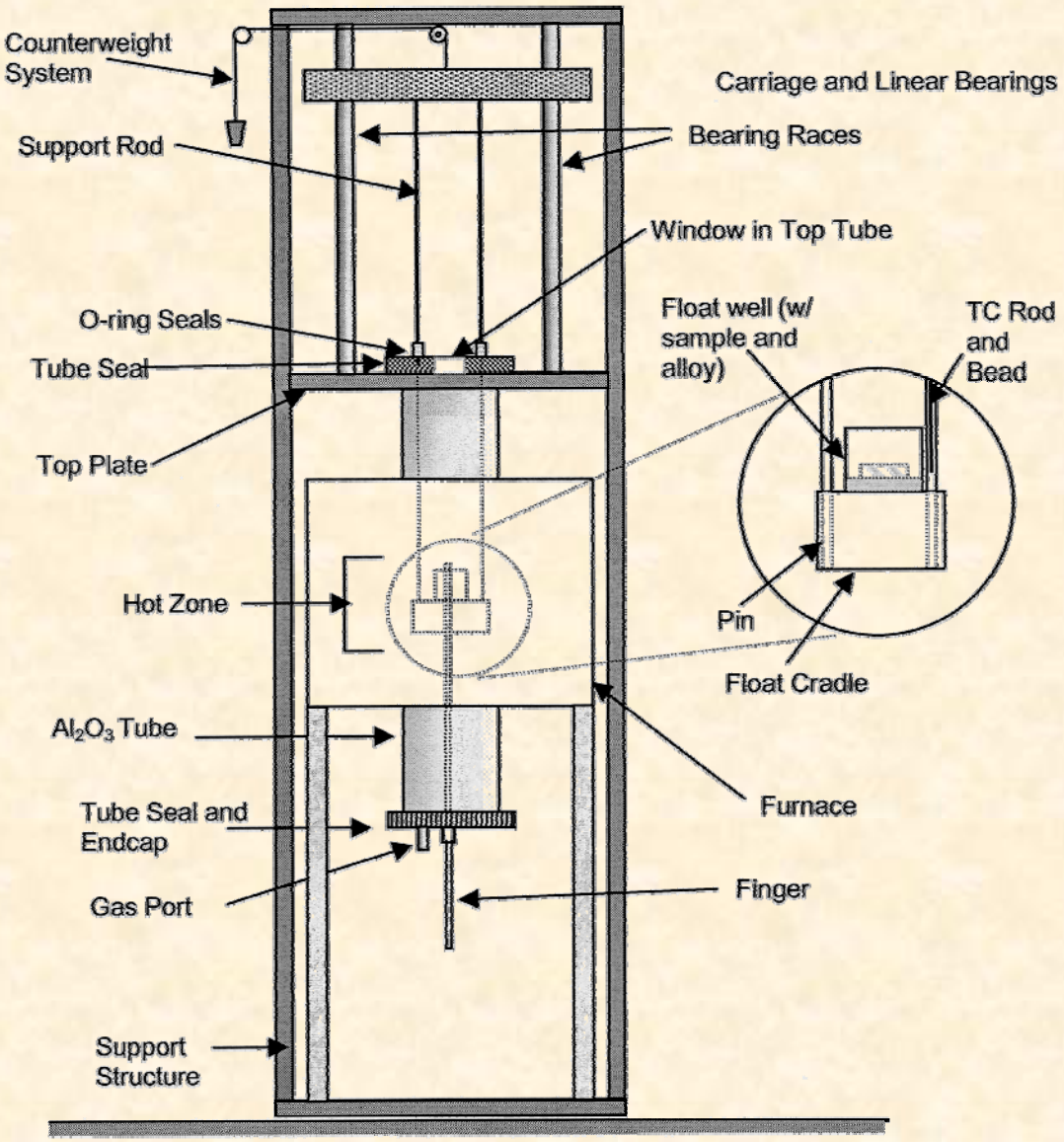


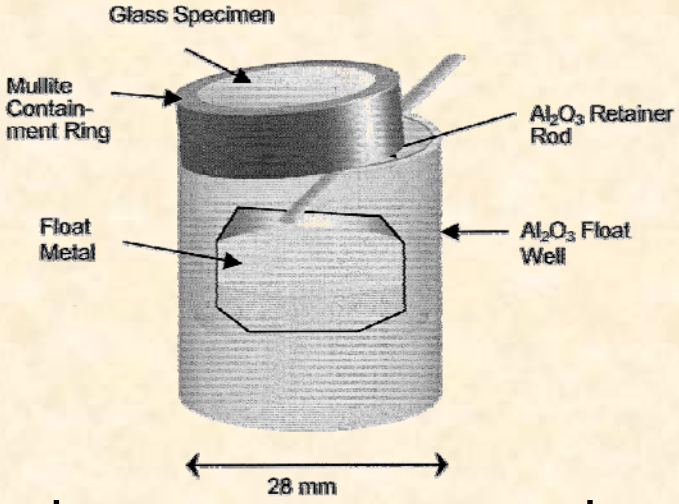


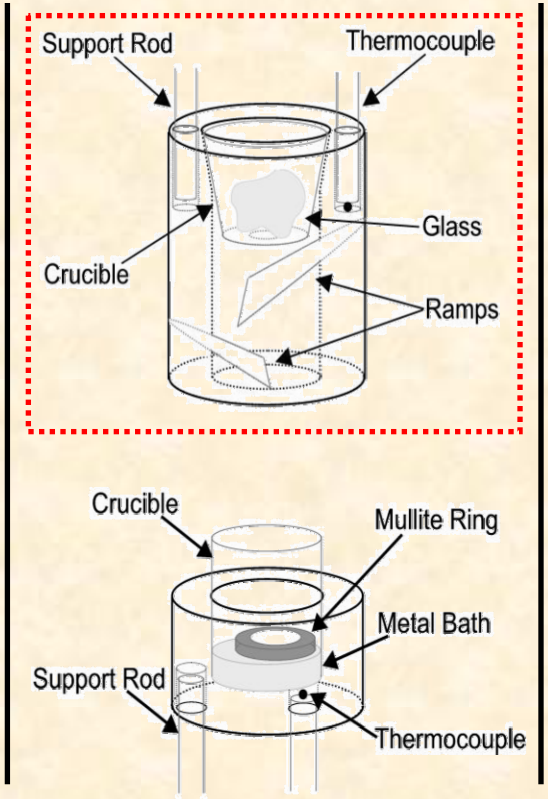


BROWN

# Dynamic Reduction in the Float-Glass Reaction

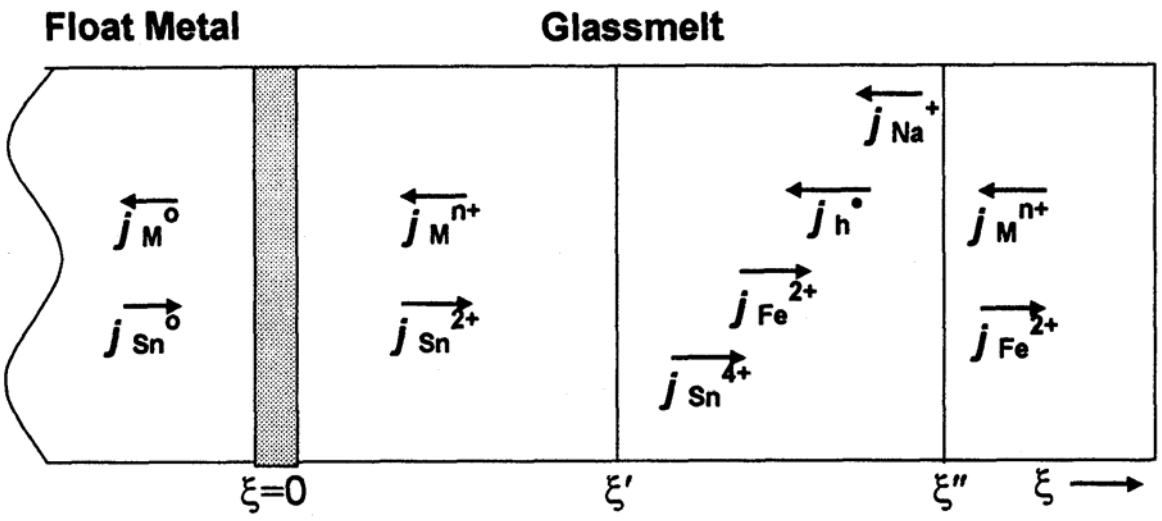


at ξ=0: $Sn^o + xSiOM = 2SiOSn_{0.5} + xM^o$

at ξ=ξ′: $2SiOSn_{0.5} + 6SiOFe_{0.33} = 4SiOSn_{0.25} + 4SiOFe_{0.5}$

at ξ=ξ″: $4SiOFe_{0.5} + (4SiOSi + 2SiOFe_{0.5} + 2NaFeO_2) = 6SiOFe_{0.33} + 6SiOFe_{0.5} + 2SiONa$

**Controlling the activity of Sn through use of an exothermic alloying with Au allows the dynamic to be manipulated, and allows, too, moving the temperature much higher.**

**Can creative co-design of silicate & metal melts allow creation of surface regions with unique properties?**

**Dynamic involves simultaneous reduction and solution-formation reactions: that these can occur at different rates allows "structural" gradients.**

BROWN

# Approach: Glass-Ceramic-Forming Silicate Melt & Multiply Oxidizable Metal Alloy

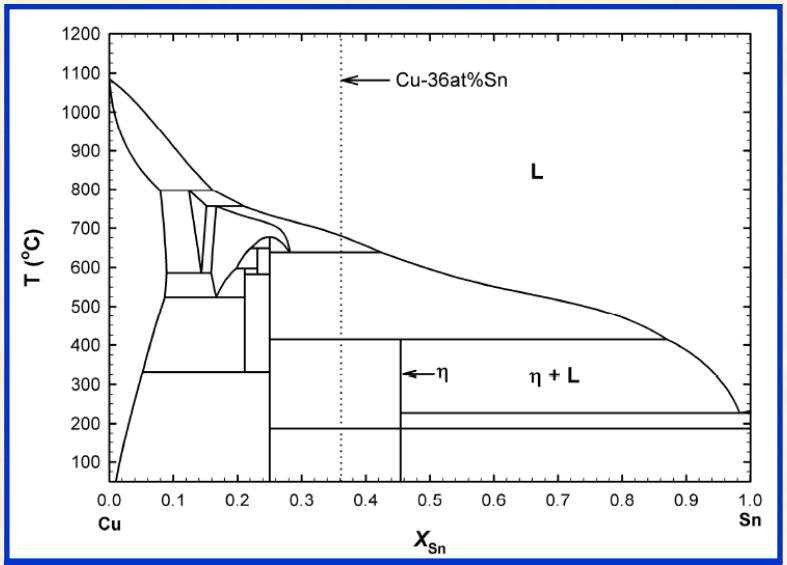


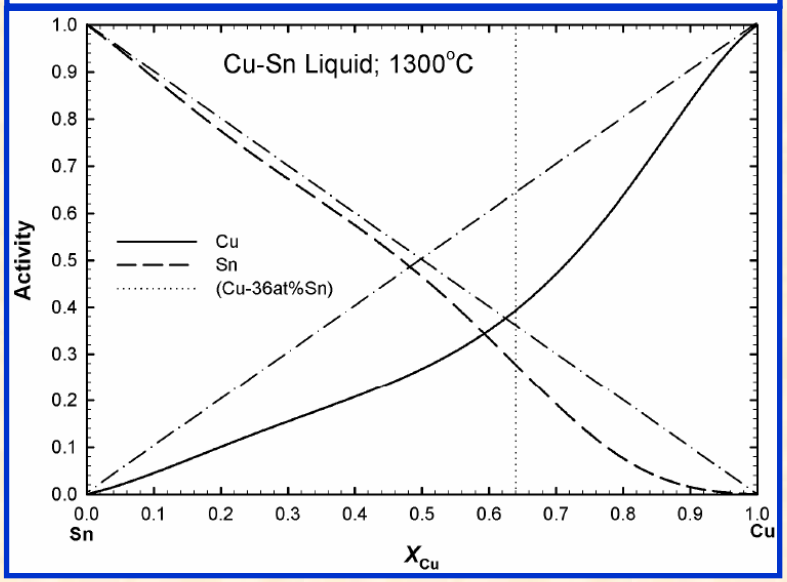


$$\left|\Delta^{o}G_{SnO}\right| > \left|\Delta^{o}G_{Cu_2O}\right|$$

## Spinel Glass-Ceramic Compositions

| | MAS | | | Zn-MAS | | |
|---|---|---|---|---|---|---|
| | oxide | | ion | oxide | | ion |
| | wt. %† | mol. %‡ | at. %‡ | wt. %† | mol. %‡ | at. %‡ |
| $SiO_2$ | 62.36 | 67.19 | 21.03 | 61.46 | 66.57 | 20.86 |
| $Al_2O_3$ | 27.45 | 17.43 | 10.91 | 27.10 | 17.30 | 10.84 |
| MgO | 9.53 | 15.30 | 4.79 | 8.47 | 13.68 | 4.29 |
| CaO | 0.06 | 0.07 | 0.02 | 0.06 | 0.07 | 0.02 |
| $Fe_2O_3$ | 0.030 | 0.012 | 0.008 | 0.150 | 0.061 | 0.038 |
| MnO | 0.006 | 0.005 | 0.002 | 0.006 | 0.006 | 0.002 |
| ZnO | — | — | — | 2.24 | 1.79 | 0.56 |
| $Na_2O$ | — | — | — | 0.49 | 0.52 | 0.32 |
| $O^{2-}$ | | | 63.24 | | | 63.07 |

**Liquid Bronze Float Alloy: Cu-36at% Sn**

BROWN

# Reduction and Mobilization of Ionic Si (1):

## *Rapid Incorporation and "Release" of $Cu^{+,2+}$*

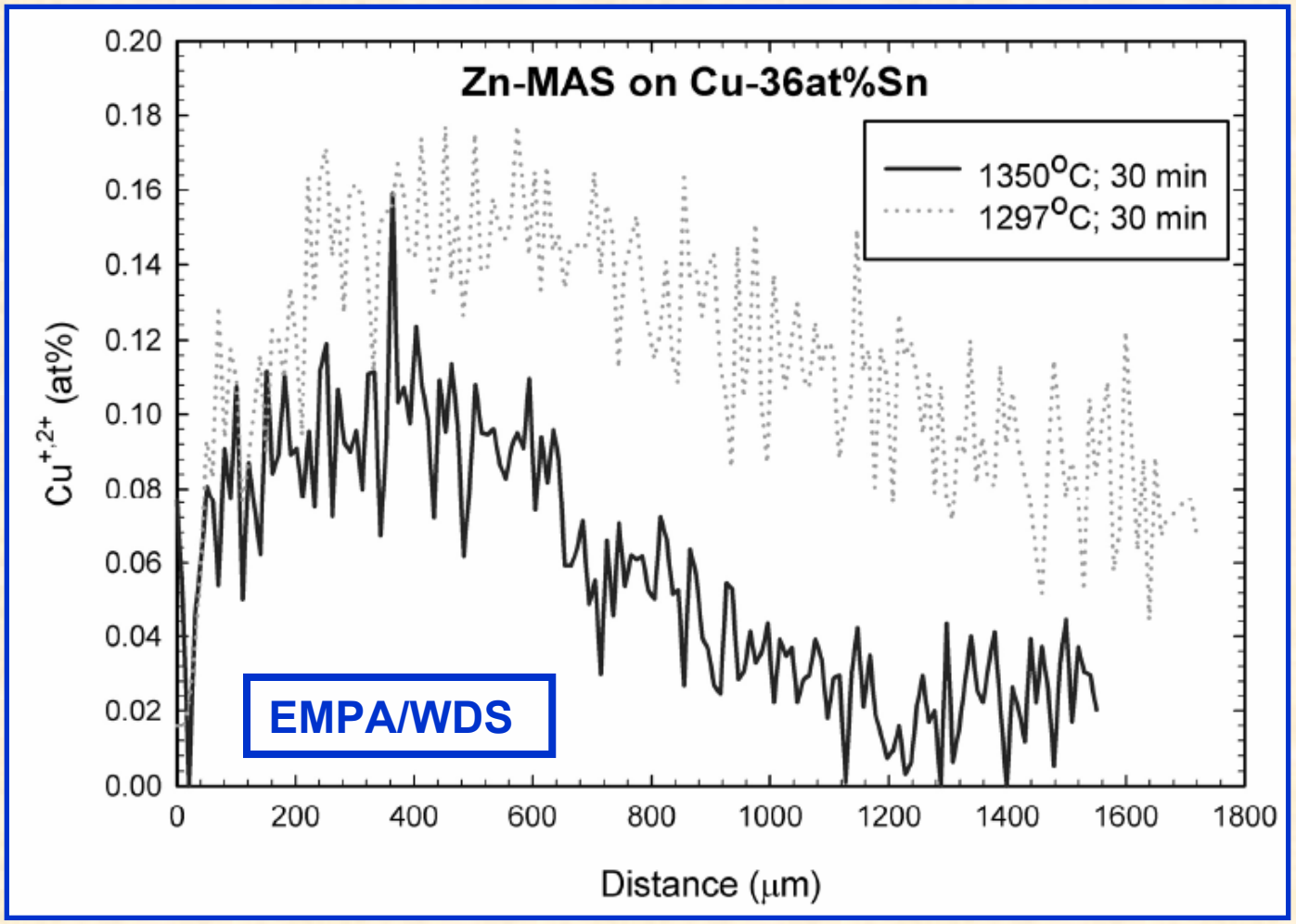


BROWN

# Reduction and Mobilization of Ionic Si (2):

## *Including Redox Couples involving $Sn^{2+,4+}$ & $Zn^{+,2+}$*

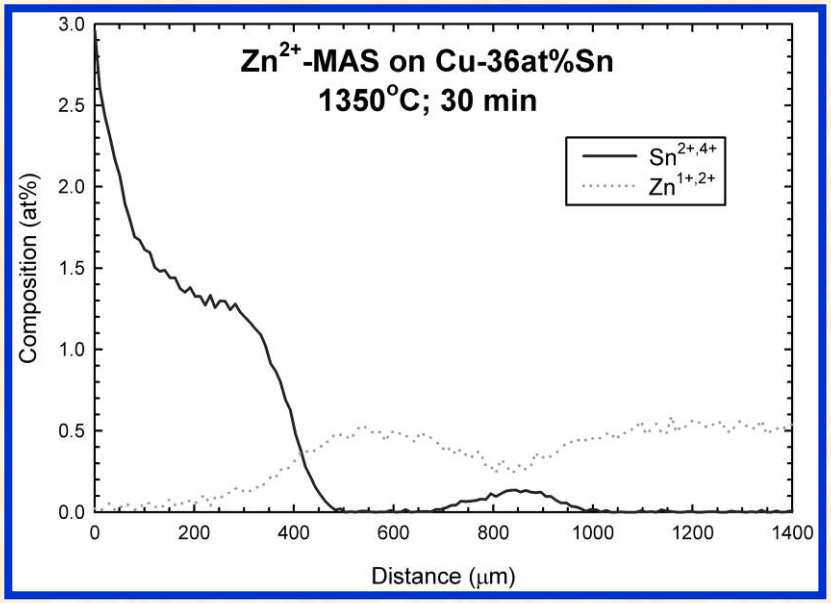


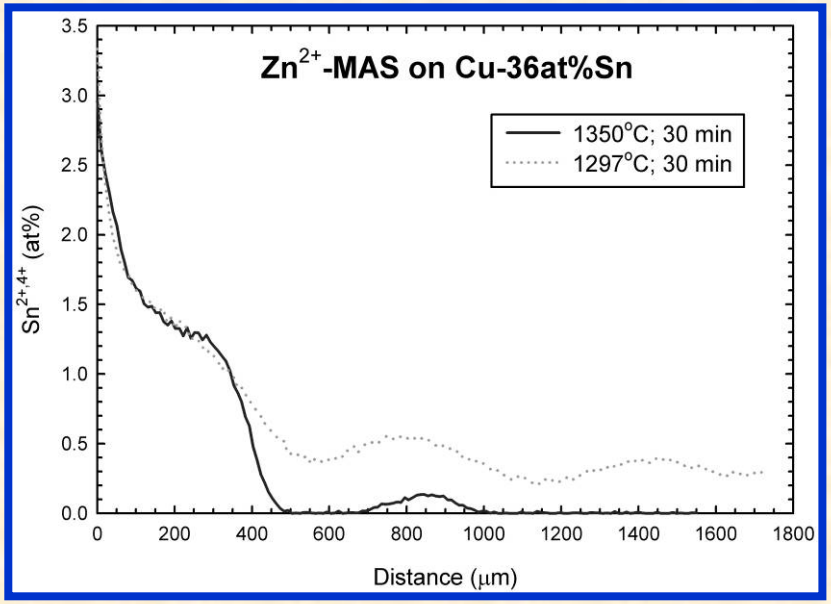


**Reduction/solution reaction clearly involves mobilization of ionic Si and Zn out of the silicate melt; transport coefficient consistent with $Si^{2+}$.**

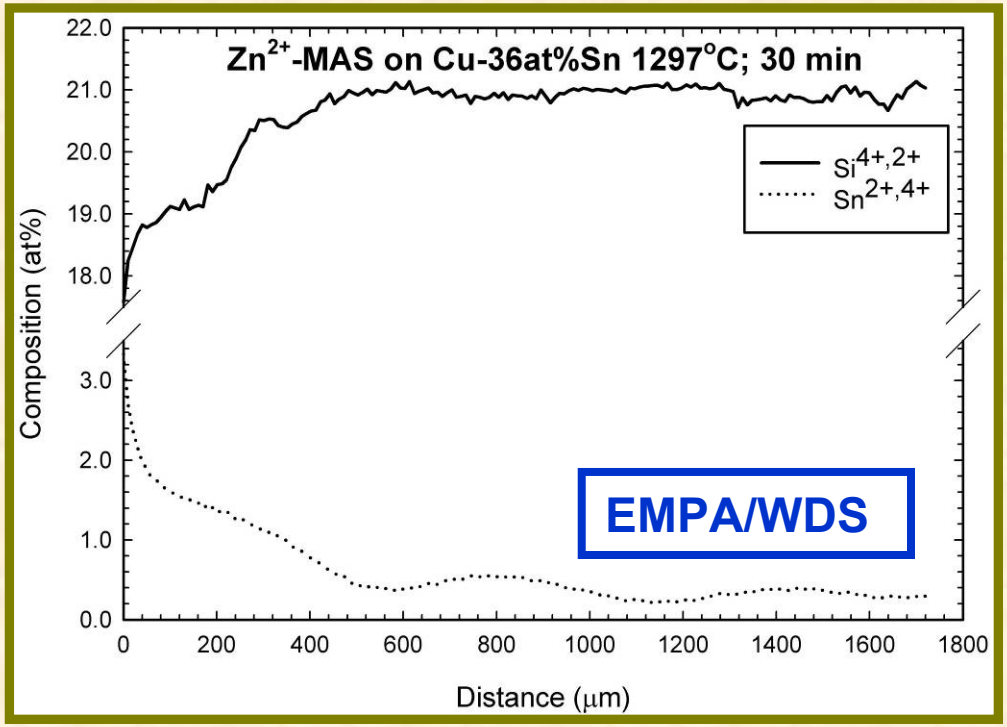


| ZnMAS | | | | | | | | |
|---|---|---|---|---|---|---|---|---|
| oxide | $SiO_2$ | $Al_2O_3$ | $Fe_2O_3$ | ZnO | MnO | MgO | CaO | $Na_2O$ |
| wt% | 61.33 | 27.01 | 0.14 | 1.80 | 0.01 | 8.43 | 0.06 | 0.47 |
| mol% | 66.86 | 17.35 | 0.06 | 1.45 | 0.01 | 13.70 | 0.07 | 0.50 |

BROWN

# Reaction Dynamics: Zn-MAS on Cu-36at% Sn

**Reaction dynamic couples $Sn^{2+,4+}$ mobility with that of $Si^{2+}$ and $Zn^{+,2+}$; the latter results in Leisegang Bands at "depth."**

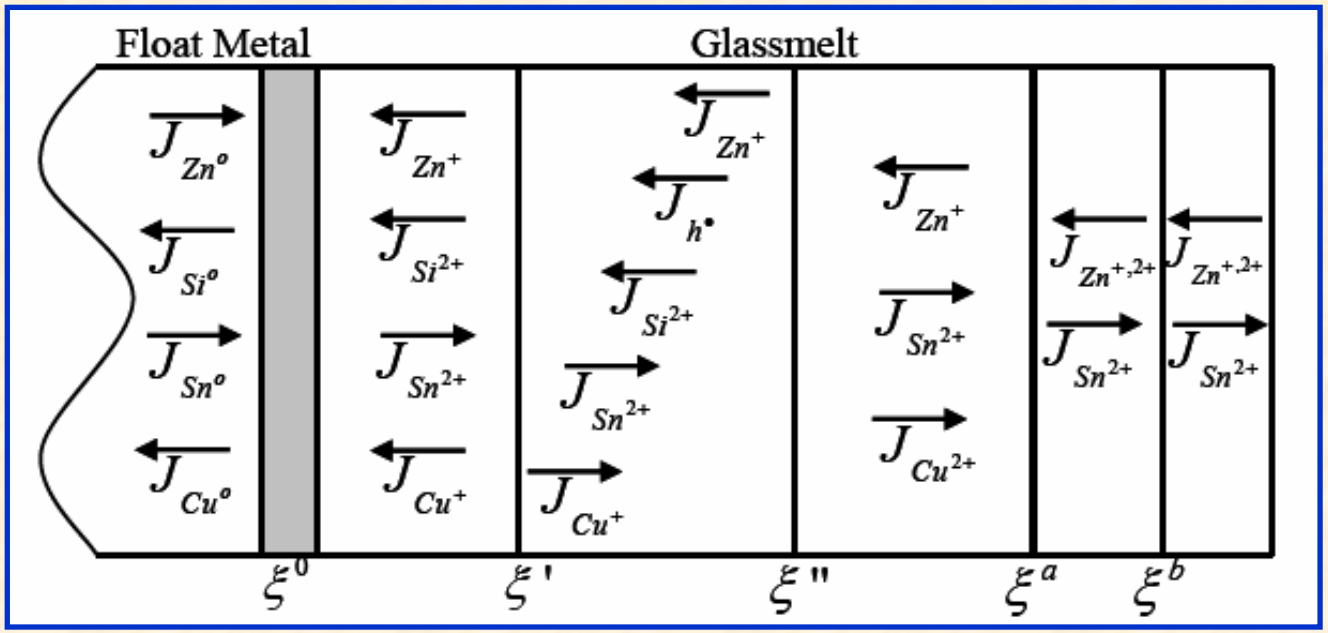


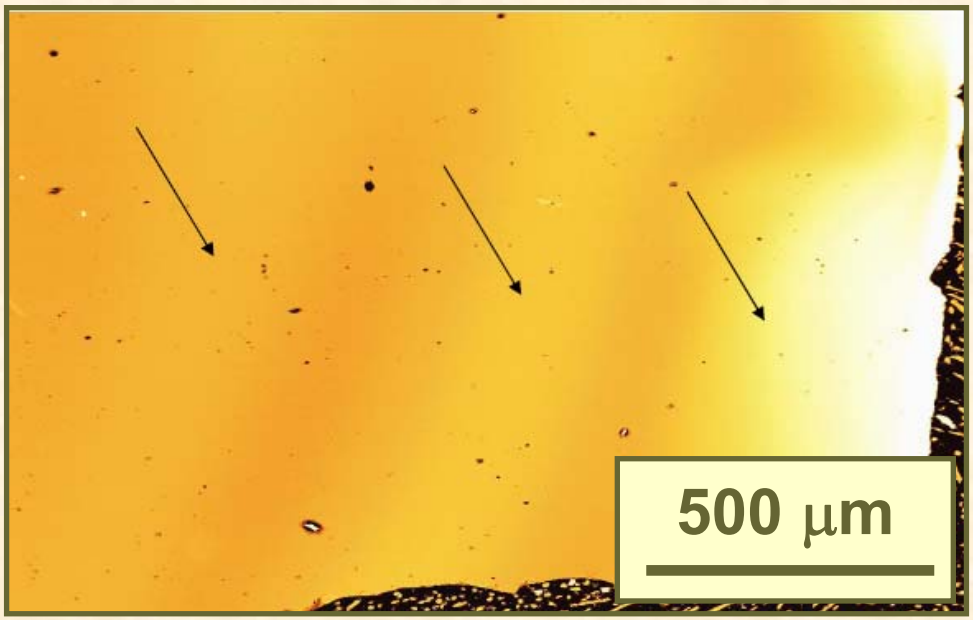


**XES Map for Sn**
**1297°C; ½ h**

BROWN

# Summary/Conclusions

1. Dynamic oxidation or reduction of a transition-metal-cation-bearing ionic melt or glass does *not* *a priori* require the diffusive motion of an oxygen species: rapidly moving electronic species (polarons: $h^{\bullet}$ or e') decouple the motions of cations from anions and other cations such that a variety of *kinetically parallel* responses are possible.

2. Kinetic parallel responses allow a reacting system to "explore" a variety of paths on the thermo-dynamic "landscape," which can lead to spatial & temporally persistent, metastable states.

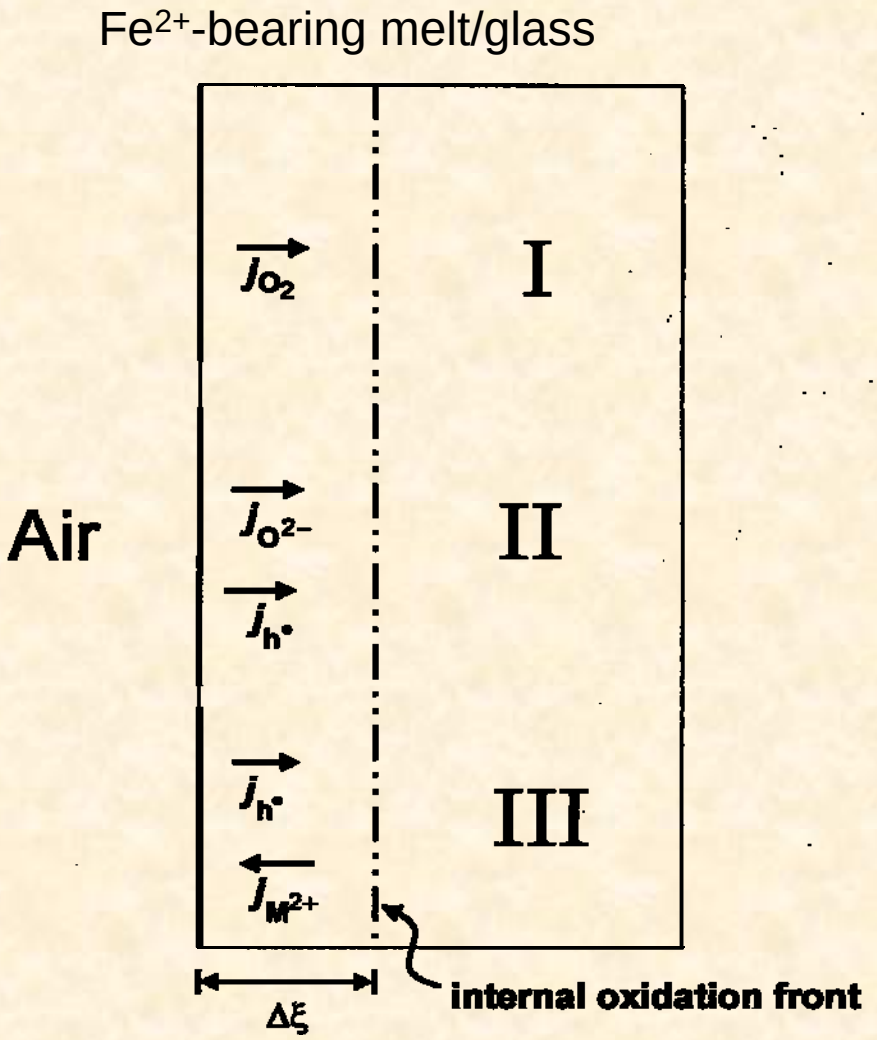


BROWN

# Summary/Conclusions (continued)

3. Dynamic redox experiments provide evidence for a number of structure/chemistry/dynamics relationships in amorphous aluminosilicates; these can perhaps be exploited for engineering purposes. Such exploitation essentially involves designing the thermodynamic landscape via chemistry: in the float process, we can design chemically both the glass-melt and the alloy float medium, affecting both the driving force and the transport coefficient(s).

4. Solution models emphasizing polymerization seem a fruitful approach to describing a "point-defect" thermodynamics in the amorphous state. Prediction in dynamics becomes possible.

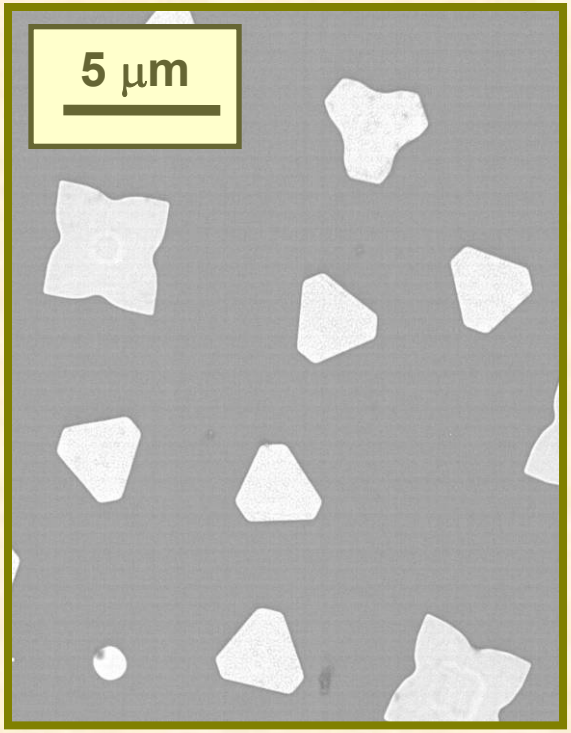


Fe-MAS; 1380°C; 10 min; $a_{O2} = 10^{-13}$

BROWN